Thesis for the Degree of Master of Engineering

Comparative Analysis of On-board Methane and Methanol Reforming Systems combined with HT-PEM Fuel Cell for Hydrogen Fueled Ship Application

Hyun Yong Lee

August, 2020

Department of Marine Systems Engineering
Graduate School
Korea Maritime and Ocean University

Comparative Analysis of On-board Methane and Methanol Reforming Systems combined with HT-PEM Fuel Cell for Hydrogen Fueled Ship Application

by

Hyun Yong Lee

Advised by

Prof. Ho Keun Kang

A Thesis Submitted to the Graduate School of
Korea Maritime and Ocean University in the partial fulfillment
Of the requirements for degree of
Master of Engineering

2020. 07. 10

Dissertation Committee

Chairman Ph.D. Tae Woo Lim

Member Ph.D. Ji Woong Lee

Member Ph.D. Ho Keun Kang

Contents

Table Contents

Figure Contents

Comparative Analysis of On-board Methane and Methanol Reforming Systems combined with HT-PEM Fuel Cell for Hydrogen Fueled Ship Application

Hyun Yong Lee

Department of Marine Systems Engineering
Graduate School of
Korea Maritime and Ocean University

Abstract

The International Maritime Organization (IMO) assessed that international shipping accounted for about 2.2% of total carbon dioxide emissions in 2012, which is approximately 796 million tonnes of CO_2, and forecasted that this amount will increase between 50% and 250% in the period to 2050 under a business-as-usual scenario. As an efforts to reduce harmful emissions from shipping industry, in April 2018, the International Maritime Organization adopted an initial strategy to reduce the total annual greenhouse gas (GHG) emissions at least 50% by 2050 compared to 2008. Several alternatives to reduce GHG was proposed which include using carbon neutral fuel such as hydrogen, ammonia etc., increasing energy efficiency of engines, adopting waste heat recovery systems and other energy converters such as fuel cell. In this study, fuel cell as an alternative energy converter for marine application was investigated.

The advantage of fuel cells for maritime applications is the reduction of noise, vibrations, and infra-red signatures, along with their modular and flexible design,

water generation, etc., although they may be application specific.

However, there are significant huddle which fuel cell has to overcome, and that is how to store fuels onboard safely. Both compressed hydrogen and liquefied hydrogen have disadvantages such as low volumetric energy density, high pressure(250~300bar for compressed H_2) and cryogenic temperature(-253℃ for liquefied H_2). Therefore in this study, fuel cell system using LNG or methanol as primary fuel, which both are being used as marine fuel, was considered.

Steam methane reforming system fed by LNG and steam methanol reforming system fed by methanol, which both are combined with HT-PEMFC system for use in hydrogen-fueled ships was modeled in Aspen HYSYS environment.

Exergy and energy analysis were implemented for comparison of systems. The required space for the primary fuel and the fuel cost have also been investigated to find the more advantageous system for ship application. All the simulations have been conducted at a fixed net electricity (Wnet,electrical : 475kW) to meet the average shaft power of the reference ship. Results show that at the base condition, the electrical efficiency of the methanol-based system are 9.37% higher than those of the methane-based system. The cogeneration efficiency of the methane-based system is 4.23% higher than that of the methanol-based system. The comparison of space for fuel reveals that the methanol-based system requires a space 1.07 times larger than that of the methane-based system for the total voyage time, although the methanol-based system has higher electrical efficiency. In addition, the methanol-based system has a fuel cost 1.07 times higher than that of the methane-based system to generate 475kW net of electricity for the total voyage time.

KEY WORDS: Hydrogen, Fuel Cell, LNG, Methanol, Reforming

수소연료선박 적용을 위한 고온형 고분자 전해질 연료전지와 통합된 메탄 및 메탄올 개질 시스템의 비교 분석

이 현 용

한국해양대학교 대학원
기관시스템공학과

초 록

국제해사기구(IMO)는 제3차 온실가스 연구 보고서를 통해서 2012년 선박기인 이산화탄소 배출량이 전 세계 이산화탄소 배출량의 약 2.2%인 2억 7,800만 톤이며, 2050년에는 이 비율이 약 50%에서 250%까지 증가할 것으로 예측하였다. 이에 따라, 2018년 4월, 국제해사기구는 해운업계의 온실가스(GHG) 배출량을 줄이기 위한 노력의 일환으로 2008년 대비 2050년까지 선박 기인 연간 온실가스(GHG) 배출량을 최소 50%까지 줄이기 위한 초기전략을 채택하였다. 온실가스 감축을 위한 몇 가지 대안으로는 수소, 암모니아 등과 같은 탄소 중립 연료 사용, 엔진의 에너지 효율 증가, 폐열 회수 시스템 도입 및 연료전지 등과 같은 새로운 에너지 컨버터의 도입 등이 대안으로 제시되고 있다.

연료전지를 선박에 적용할 경우, 연료전지의 종류와 용도에 따라 다를 수 있지만, 모듈식 설치에 따른 공간효율성, 소음 및 진동의 최소화 등이 장점으로 꼽힐 수 있다.

하지만, 연료전지를 선박에 적용하기 위해서는 극복해야 할 과제들이 많이 있으며, 이 중 하나가 바로 연료를 안전하고 효율적으로 선박에 저장하는 방법이다. 압축수소와 액체수소는 부피 에너지 밀도가 기존 선박연료 대비 낮다는 단점을 가지고 있으며, 액체수소의 경우, -253℃의 극저온, 압축수소의 경우,

250~350bar의 고압저장에 따른 위험성이 단점으로 꼽히고 있다. 하지만 이 중에서도 선박의 공간제약성을 고려하면, 낮은 부피 에너지 밀도가 가장 큰 단점으로 고려된다. 따라서 본 연구에서는 기존에 선박 연료로 사용되고 있는 LNG 또는 메탄올을 1차 연료로 사용하는 연료전지시스템을 고려하였다.

고온형 고분자 전해질 연료전지 시스템과 결합된, LNG를 1차 연료로 사용하는 수증기-메탄 개질시스템과 메탄올을 1차 연료로 사용하는 수증기-메탄올 개질시스템이 각각 Aspen HYSYS에서 모델링되었다.

시스템 성능 분석을 위해 엑서지 및 에너지 분석기법이 적용되었으며, 나아가 선박 적용에 보다 유리한 시스템을 찾기 위해 1차 연료에 필요한 공간 및 연료 비용 분석을 수행하였다. 모든 시뮬레이션은 본 연구에 적용된 기준 선박의 평균 샤프트 출력을 만족하기 위해 고정전력 (W_{net} : 475kW)을 고려하여 수행되었다.

시뮬레이션 결과, 기본 설계조건에서 메탄올 기반 시스템의 전기 효율이 메탄 기반 시스템의 전기 효율보다 9.37% 높으며, 메탄 기반 시스템의 열병합 효율이 메탄올 기반 시스템의 열병합 효율보다 4.23% 더 높게 나타났다.

1차 연료의 저장 부피 분석을 통해서, 메탄올 기반 시스템이 더 높은 전기 효율을 갖지만, 메탄올 기반 시스템이 총 항해 시간 동안 메탄 기반 시스템보다 1.07배 더 큰 공간을 필요로 하는 것으로 나타났다. 또한, 메탄올 기반 시스템은 총 항해 시간 동안 475kW의 전기를 생성하기 위해 메탄 기반 시스템보다 1.07배 높은 연료 비용을 갖는 것으로 나타났다.

KEY WORDS: 수소, 연료전지, 액화천연가스, 메탄올, 개질

Chapter 1 Introduction

1.1 Background

The International Maritime Organization assessed that international shipping accounted for about 2.2% of total carbon dioxide emissions in 2012, which is approximately 796 million tonnes of CO_2, and forecasted that this amount will increase between 50% and 250% in the period to 2050 under a business-as-usual scenario [1]. However, when the Paris Agreement on climate change mitigation was adopted in 2015 to deal with the global-warming concerns, shipping was not included [2]. Instead, in April 2018, the IMO established a strategy to reduce the total amount of annual greenhouse gas (GHG) emissions from shipping by at least 50% by 2050 compared to 2008 [3].

To be specific, in April 2018, 72nd of IMO's Marine Environment Protection Committee (MEPC) adopted resolution MEPC.304(72) as an Initial IMO Strategy on reduction of GHG emissions from ships (IMO GHG Strategy). The vision of the IMO GHG Strategy confirms IMO's commitment to reducing GHG emissions from international shipping and, as a matter of urgency, to phasing them out as soon as possible in this century. Level of ambition directing the IMO GHG Strategy are to following;

① review with the aim to strengthen the energy efficiency design index (EEDI) requirements for new ships with percentage improvement for each phase to be determined for each ship type,

② reduce CO_2 emissions per transport work, as an average across international shipping, by at least 40% by 2030, pursuing efforts towards 70% by 2050, compared to 2008,

③ peak GHG emissions from international shipping as soon as possible and to

reduce the total annual GHG emissions by at least 50% by 2050 compared to 2008.

The IMO GHG Strategy sets out candidate short- (2018-2023), mid- (2023-2030) and long-term (beyond 2030) further measures of the IMO on matters related to the reduction of GHG emissions from ships. Therefore, technologies to meet IMO's goal in shipping sector is being discussed.

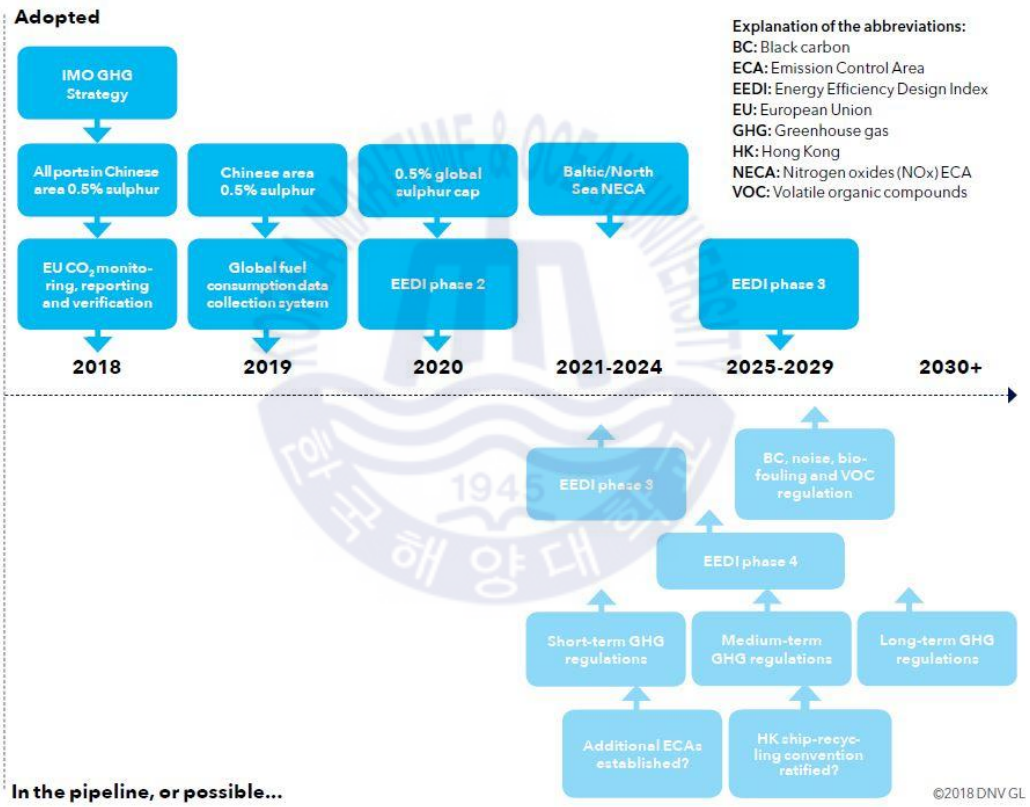

Fig. 1 IMO GHG Strategy [2]

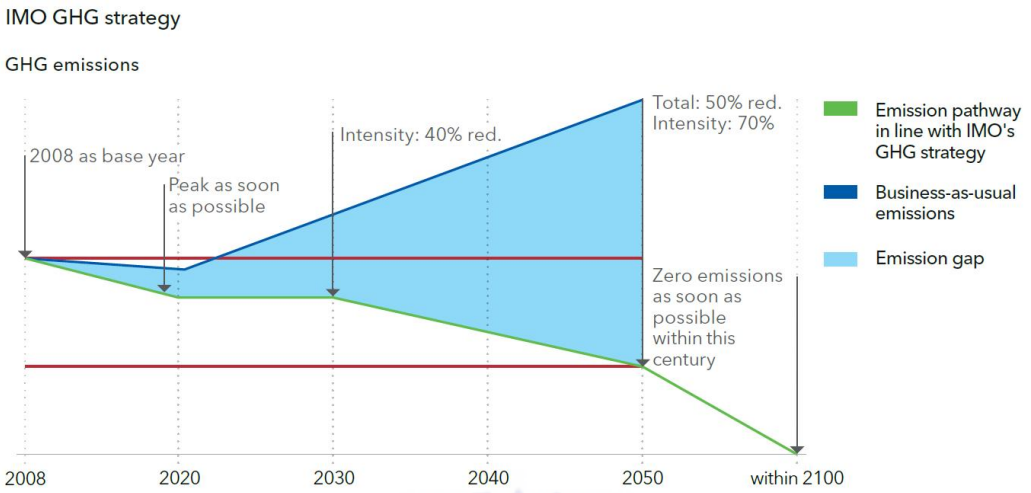

Fig. 2 Timeline of environmental regulations towards 2030 [2]

1.2 Fuel Cells as Alternative Solutions

In order to achieve low carbon pathways, several technical and operational measures that improve energy efficiency and reduce CO_2 emissions in the shipping industry should be introduced, such as increasing energy efficiency of engines, adopting waste heat recovery systems, improving the hull form, implementing speed reduction and alternative sea routes [4]. In addition to the above measures, using different propulsion systems, such as fuel cells, are also considered possible alternatives [5]. Hydrogen fuel cells emit no direct GHGs, but the emissions generated during hydrogen production should be considered. The emissions from hydrogen production are highly dependent on feedstock and primary energy sources [6]. In the shipping industry, fuel cell power generation can eliminate NOx, SOx, and particulate material (PM) emissions, and reduce CO_2 emission compared to emissions from conventional diesel engines [2]. The advantage of fuel cells for maritime applications is the reduction of noise, vibrations, and infra-red signatures, along with their modular and flexible design, water generation, etc., although they

may be application specific [5]. However, the most significant huddle which fuel cell to overcome is the availability of fuels, namely how to store fuels onboard safely.

1.3 Objective and Scope

Author in this study consider, to achieve zero emission from shipping, alternative fuels such as green hydrogen from renewable energy should be applied. However, storage volume for hydrogen, lack of infrastructure for hydrogen bunkering and higher cost of hydrogen etc. are challenging at the current level of technology. Therefore, on-board steam reforming integrated with fuel cell could be one of transition solutions. In this study, author present on-board methane and methanol steam reforming system integrated with HT-PEMFC system for power generation of ships. Performance of the integrated systems were evaluated by exergy and energy analysis. In addition, spaces required for primary fuel storage were also compared. Those evaluations were carried out for a reference ship. The features of this study distinguished from other researches are as follows :

(1) Steam reforming, HT-PEMFC systems are simultaneously considered. Heat integration and recovery were implemented for practical comparison.

(2) For steam methane reforming-based system, liquefied natural gas (LNG) was used as primary fuel since it is most cost effective manner for ship storage of natural gas and well proved in LNG fueled ship application.

The main objectives of this study are as follows:

(1) To develop methane and methanol steam reforming systems combined with HT-PEMFC system which are suitable for reference ship.

(2) To carry out exergy and energy analyses for the developed, integrated systems to assess the energy efficiency, exergy efficiency and exergy destruction of components within each system.

(3) To evaluate overall fuel cost and overall space required for storage of the primary fuels.

(4) To carry out parametric studies with varying operating conditions, such as the S/C ratio, operating temperature of the reforming process.

Chapter 2 Overview of Fuel Cell and Steam Reforming System

2.1 Fuel Cell Technologies

Fuel cells directly convert chemical energy in fuels to electrical energy and heat by electrochemical processes. Since electrochemical processes is not subject to Carnot's law, fuel cell systems have relatively higher efficiencies resulting low pollutant emissions. Fig. 1 illustrates the schematic of Proton Exchange Membrane Fuel Cell (PEMFC).

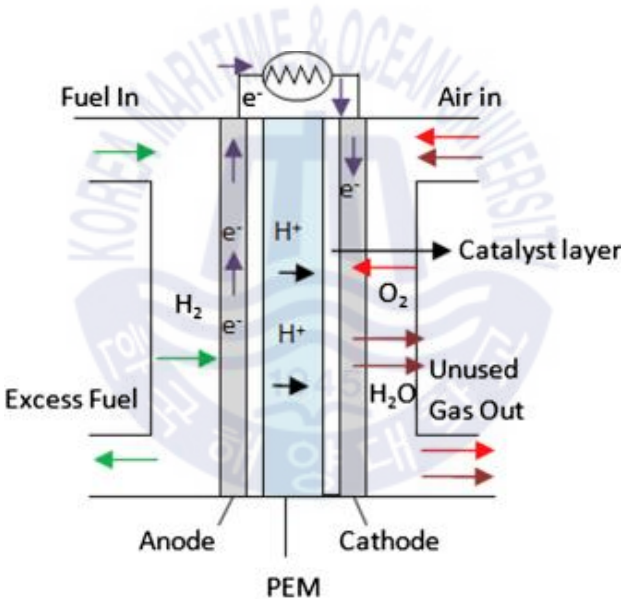

Fig. 3 Schematic of PEMFC

The several fuel cell demonstration project for ship application was carried out worldwide. Almost various fuel cell types and different fuels such as hydrogen, liquefied natural gas (liquefied), liquefied pressurized gas (LPG), methanol, and maritime diesel have been considered. Those project are listed in table 1.

Table 1 Fuel cell projects worldwide [7]

Project	Concept	Fuel Cell	kW	Fuel
FellowSHIP	Auxiliary power of Offshore Supply Vessel	MCFC	320kW	LNG
Viking Lady METHAPU Undine	20 kW SOFC tested for marine APU.	SOFC	20kW	Methanol
E4Ships – Pa-X-ell MS MARIELLA	Decentralized auxiliary power supply onboard passenger vessel MS MARIELLA.	HT-PEM	60kW	Methanol
E4Ships - SchIBZ MS Forester	100 kW containerized SOFC system for the auxiliary power supply of comercial ships.	SOFC	100kW	Diesel
E4Ships - Toplanterne	Support of IGF Code development	-	-	-
RiverCell	Tested for a hybrid power supply for river cruice vessles	HT-PEM	250kW	Methanol
RiverCell – Elektra	Feasibility study for a fuel cell as part of a hybrid power supply for a towboat	HT-PEM	-	Hydrogen
ZemShip - Alsterwasser	100 kW PEMFC system developed and tested onboard of a small passenger ship	LT-PEM	96kW	Hydrogen
FCSHIP	Assess the potential for maritime use of FC	MCFC SOFC LT-PEM	-	Various
New-H-Ship	Research project on the use of hydrogen in marine applications	-	-	-
Nemo H2	Small passenger ship in the canals of Amsterdam	LT-PEM	60kW	Hydrogen
Hornblower Hybrid	Hybrid ferry with diesel generator, batteries, PV, wind and fuel cell	LT-PEM	32kW	Hydrogen

Hydrogenesis	Small passenger ship which operates in Bristol	LT-PEM	12kW	Hydrogen
MF Vagen	Small passenger ship in the harbour of Bergen	HT-PEM	12kW	Hydrogen
Class 212A/214 Submarines	Hybrid propulsion using a fuel cell and a diesel engine	LT-PEM	-	Hydrogen
US SSFC	Fuel cell power systems that will meet the electrical power needs of naval platforms	LT-PEM MCFC	500kW (PEM) 625 kW (MCFC)	Hydrogen
SF-BREEZE	Feasibility study of a high-speed hydrogen fuel cell passenger ferry	LT-PEM	Total power 2.5MW	Hydrogen
MC-WAP	The application of FC technology onboard large vessels	MCFC	500kW	Diesel
FELICITAS –subproject 2	Mobile hybrid marine version of the Rolls- Royce Fuel Cell SOFC system	SOFC	250kW	LNG,
FELICITAS –subproject 3	PEMFC-Cluster	LT-PEM	Cluster system	HC and hydrogen
FELICITAS –subproject 4	Power management-concerns general technical problems of FC-based propulsion	LT-PEM	-	-
Cobalt 233 Zet	Sports boat employing hybrid propulsion	LT-PEM	50kW	Hydrogen

Seven fuel cell types were evaluated from the perspectives of relative cost, module power level, lifetime, tolerance for cycling, flexibility towards type of fuel, technological maturity, size, sensitivity to fuel impurities, emissions, safety, and efficiency. As a result of the evaluation, the low temperature proton exchange membrane (LT-PEMFC) and the high temperature proton exchange membrane fuel cell (HT-PEMFC) received, respectively, the first and second highest score in the ranking, and this implied that those technologies are the most promising for marine

use [7]. In the following sections, those fuel cells will be explained.

2.1.1 LT-PEMFC

The LT-PEMFC is a mature technology that has been successfully applied both in marine and other high energy applications. The operation requires pure hydrogen, and the operating temperature is low [7]. Hydrogen can be generated by on-board reforming with additional equipment or by storing compressed or liquid hydrogen on board. Its main reactions are as following.

Anode reaction:

$$2H_2 = 4H^+ + 4e^- \quad (1)$$

Cathode reaction:

$$O_2 + 4H^+ + 4e^- = 4H_2O \quad (2)$$

Total reaction:

$$2H_2 + O_2 = 2H_2O \quad (3)$$

The LT-PEMFC uses platinum-based electrodes and the electrolyte is a humidified polymer membrane. Electrolyte polymer membrane between the cathode and anode is used to only allow protons [H+] to pass through and is commonly made of a material called Nafion [8]. The operating temperature is 50-100°C and temperatures above 100°C is not feasible as the electrolyte polymer membrane needs to stay humid [7]. However, due to its low temperature operation, the electrochemical reaction's kinetics are hindered and therefore, it is necessary to employ electrocatalyst materials such as platinum [9] which lead to a higher cost of LT-PEMFC. Furthermore, lower operational temperature of LT-PEMFCs result in the limited tolerance to fuel impurities such as sulfur and carbon monoxide (CO), which reduce its performance drastically.

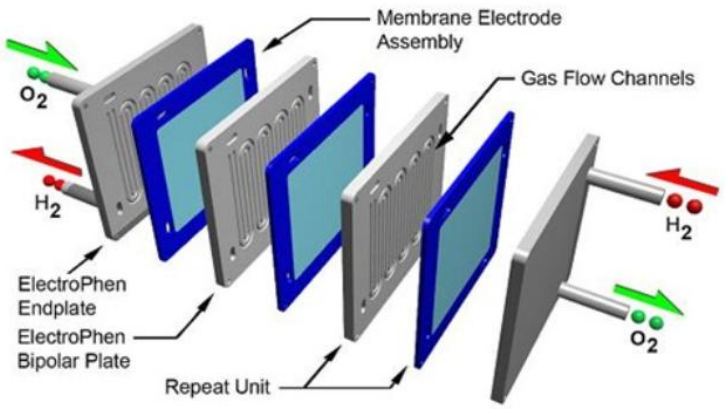

Fig. 4 Components of PEMFC

The following describes some advantages of LT-PEMFC technology compared to other fuel cells [8]:

- Lower operating temperature (50~100℃)
- Faster growing industry due to demand by automobile companies
- Superior gravimetric and volumetric power specifications
- Fast start up time (0~100%) in 5~10 sec; (low~100%) less than 1 sec
- Simpler and more compact than other types of cells
- Efficiency is high, even in lower power range as can be seen in Fig.3

Although LT-PEMFC shows good transient response capabilities, if a hydrocarbon fuel with fuel processing equipment such as reformer is used, those advantage are partially reduced [5,10]. This is because reformer operate at a significantly higher temperature than the stack.

2.1.2 HT-PEMFC

The HT-PEMFC is recently developed a technology and therefore, it is less mature than conventional LT-PEMFC. The main difference between a HT-PEMFC

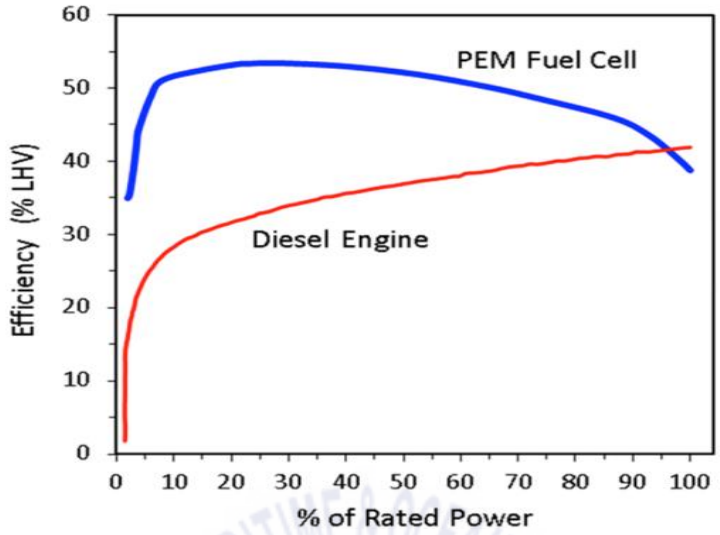

Fig. 5 Thermal efficiency of a Hydrogenics HD-30 PEM fuel cell and MTU 16v4000 diesel engine

and PEMFC is that HT-PEMFC operate at higher operating temperature, thanks to mineral acid electrolyte.

An LT-PEMFC has relatively higher power density than an HT-PEMFC; however, the HT-PEMFC has several other advantages [11]. The operating temperature of LT-PEMFCs is between 50 and 100°C and that for HT-PEMFCs is between 120 and 200°C. The higher operational temperature of LT-PEMFCs results in better tolerance to fuel impurities such as sulfur and carbon monoxide (CO), which reduce its performance drastically. To be specific, LT-PEMFCs require fuels containing less than 30 ppm of CO and less than 1 ppm of sulfur, whereas HT-PEMFCs can work with concentrations of up to 3% of CO and 20 ppm of sulfur in the fuel without permanent degradation [7]. This higher tolerance to impurities of HT-PEMFC makes it possible to develop a simpler fuel reforming system [11]. In addition, lower operating temperature of LT-PEMFC generate low quality of heat which heat recovery is not feasible, however excess heat from

HT-PEMFC can be recoverd and utilized, such as steam generation onboard.

Additionally, the water management of HT-PEMFCs is easier because the water produced in the fuel cell is in vapor, and the waste heat from HT-PEMFCs can be recovered and used for steam or hot water generation [12]. Therefore in this study, HT-PEM fuel cell system is selected for simulation.

Fig. 6 MS Mariella

Fig. 7 HT-PEMFC installed onboard MS Mariella

2.2 Steam Reforming Technologies

2.2.1 General

Since the gravimetric energy density of hydrogen is approximately 120 MJ/kg, 2.47 times higher than that of natural gas and 2.8 times higher than that of diesel, hydrogen provides higher gravimetric energy than other fossil fuels. However, volumetric energy density of liquid hydrogen is approximately 8.51 GJ/m^3, which corresponds to 40.8% of natural gas and 23.7% of diesel [13]. The lower volumetric energy density could be a drawback for some vessels in those applications that cannot support a large volume of storage or higher frequency of refueling [14]. To overcome this, several maritime fuel cell studies have considered on-board reforming of methane and methanol to hydrogen, although the applied fuel cell types are different [5,15-23]. This is because methane and methanol stored at liquid state have higher volumetric energy density than hydrogen, and the operation

expenditure (OPEX) can be reduced owing to the lower price of both fuels compared to that of hydrogen. In addition, the bunkering infrastructure for methane and methanol is not an issue, unlike that for hydrogen. The bunkering infrastructure for methane (namely LNG) is rapidly expanding, and that for methanol requires minimal modification from the existing conventional infrastructure [5,15]. Properties of fuels for comparison purpose are provided in Table 2 and Figure 6.

There are several technologies for reforming carbon-based fuels to hydrogen, which include steam reforming, partial oxidation, and auto-thermal steam reforming. Among these processes, steam reforming is most mature technology, and provides higher efficiency, higher production yield, and lower rate of side reactions [24]. In the following section, technologies of steam methane reforming and methanol reforming, respectively are introduced.

Table 2 Comparison of fuels [25]

Fuel Characteristics	**Hydrogen**	**LNG**	**Methanol**
Chemical Composition	H_2	CH_4	CH_3OH
Boiling Point, ℃ 1 bar	-253	-162	65
LHV, MJ/kg	120.2	48	19.9
Auto Ignition Temp, ℃	535	650	440
Flammable Range, % vol in air	4~74%	5~15%	6.0~36%
Energy Density, MJ/lt	9.2	21.6	15.7
Volume Comparison HFO (Energy Density)	4.33	1.85	2.54
Carbon Content	0	0.75	0.375
Carbon Content Reduction (Compared to HFO)	100%	12%	56%
CO_2, kg CO_2/kWh	0	0.2061	0.2486
CO_2, kg CO_2/kWh Reduction (Compared to HFO)	100%	26%	11%
Low Flashpoint Fuel	Yes	Yes	Yes

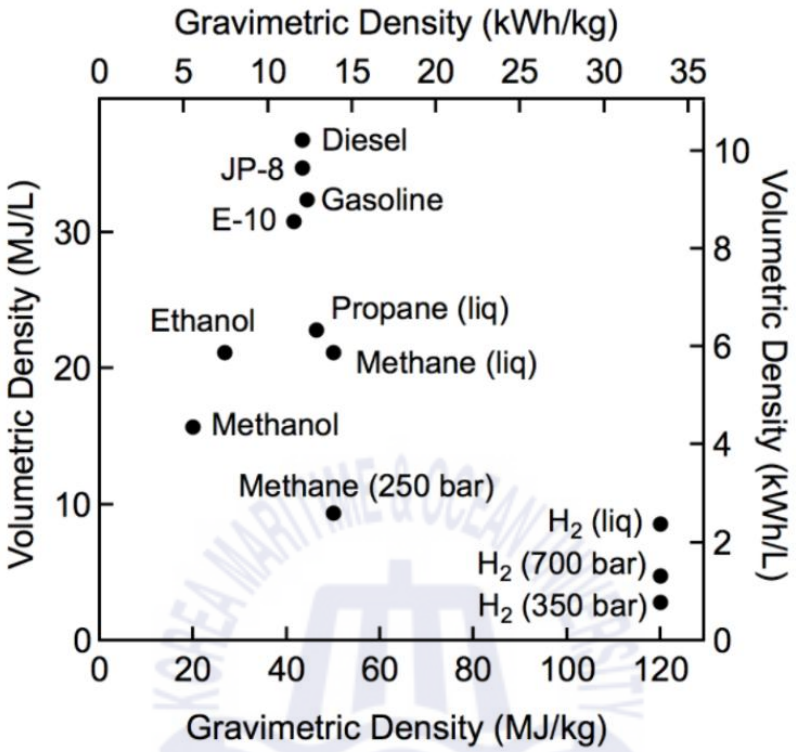

Fig. 8 Comparison of specific energy (energy permass or gravimetric density) anenergy density (energy pervolume or volumetric density) for several fuels.

2.2.2 Steam Reforming Reaction

Steam reforming uses natural gas or light hydrocarbons to produce hydrogen. Reaction is highly endothermic, and therefore, require significant source of heat such as combustor. Reaction occurs are as following:

$$C_nH_m + nH_2O = nCO + (n+0.5m)H_2 \quad (4)$$

Preferred temperatures for steam reforming varies with fuel type, i.e methane or methanol. In general, steam methane reforming is carried out at temperature between 700~1000℃ and steam methanol reforming is carried out at temperature between 200~300℃. The catalyst conventionally used in steam reforming process is based on nickel metal dispersed on oxides such as α-alumina and $MgAl_2O_4$ [26].

As can be seen in equation (4), through steam reforming reaction, carbon monoxide along with hydrogen is produced. As explained in previous section, carbon monoxide degrades performance of both LT-PEMFC and HT-PEMFC, although degree of degrade is different. Therefore CO removal process, namely water gas shift (WGS) reaction is required. Through water gas shift reaction, carbon monoxide and additional steam react and produce more hydrogen and carbon dioxide.

$$CO + H_2O = CO_2 + H_2 \quad (5)$$

A main components of reforming system are as following ;

- Reformer
- CO Clean up unit (WGS)
- Desulfurization
- Heat exchanger
- Compressor
- Pump

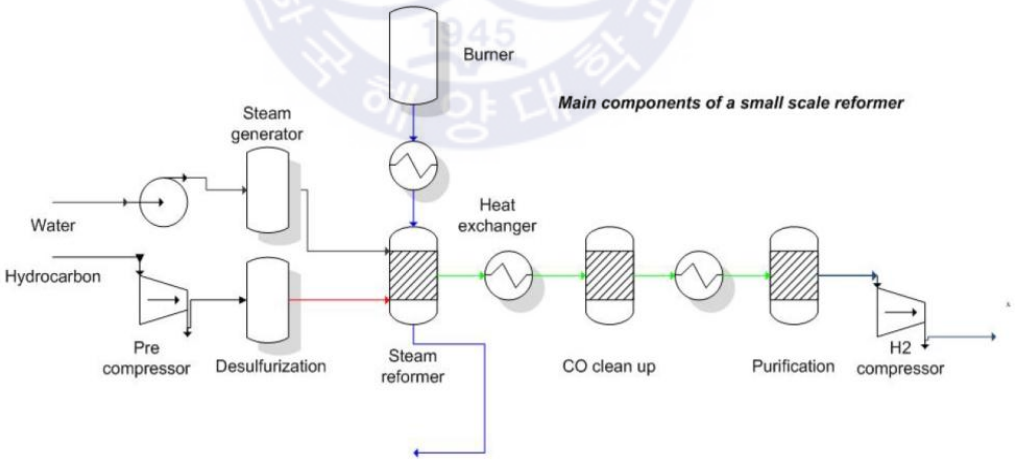

Fig. 9 Illustration of main components for steam reforming system [26]

Chapter 3 Literature Reviews

3.1 Steam Methane Reforming System and HT-PEM Fuel Cell

Steam methane reforming is one of the most proven and commercially available technologies for hydrogen production [27], and at present, 80% to 85% of global hydrogen production is derived via this technology [28,29]. Steam methane reforming technology has been widely investigated from the energy and exergy efficiency and economic and environmental perspectives in the past decades.

Simpson et al. evaluated the performance of steam methane reforming system using an exergy analysis. The results revealed that irreversibility of chemical reactions results in the largest amount of exergy destruction, and exergy loss through the exhaust gas stream was significant. Results of a parametric study show that the highest exergy efficiencies of 62.73% was achieved at operating temperatures of 974 K. The highest exergy efficiencies of 62.85% was attained at an operating pressure of 6.8 atm. The effect of steam carbon ratio (S/C ratio) was also investigated, and the result revealed that the highest efficiencies were achieved at an S/C ratio of approximately 3.2 [28]. Welaya et al. evaluated the partial oxidation and steam reforming process to convert a carbon-based marine fuel, such as natural gas, gasoline, and diesel, into hydrogen-rich gases suitable for application to the PEMFCs on board ships. Among several options evaluated, the natural gas steam reforming system showed the highest fuel processing efficiency [17]. Authayanun et al. investigated the theoretical performance of an HT-PEMFC integrated with the steam reformer using various primary fuels, i.e., methane, methanol, ethanol, and glycerol. Results revealed that for the steam methane reforming, CO fraction lower than the acceptable limit for the HT-PEMFC can be attained with higher S/C ratios and lower temperature. For S/C ratios (3~6), operating temperature lower than 1000 K should be maintained in order to keep

the CO fraction at an acceptable level for an HT-PEMFC or a water–gas shift (WGS) reactor should be included. Steam methanol reforming produces the lowest CO fraction among the studied fuels and can be directly fed to the HT-PEMFC for all of the studied cases (S/C ratio: 1~3, reformer temperature: 423~523 K). The steam methanol reforming system without a WGS reactor and steam methane reforming with a WGS reactor achieved the highest system efficiency, approximately 50%, among several options in the study [30]. Nerem et al. evaluated hydrogen, LNG, or methanol as PEMFC fuel on a cruise vessel, based on the space required on board, environmental impact, and life cycle cost (LCC) aspects. An external reformer other than hydrogen fuel was considered. Results show that the LNG system requires the smallest dimensions, whereas hydrogen and methanol require equal dimensions. From the perspective of environmental impact, LNG is a better solution than methanol for use in fuel cells. Further, LNG achieved the lowest LCC, 1.10 times higher than heavy fuel oil (HFO), while hydrogen and methanol are 1.14 and 1.15 times more expensive than HFO [15]. Arsalis et al. evaluated a micro combined heat and power system integrated with HT-PEMFC and steam methane reformer. They reported that the cogeneration and electrical efficiencies of the system are 55.46% and 27.62%, respectively [31].

3.2 Steam Methanol Reforming System and HT-PEM Fuel Cell

Methanol is an advantageous fuel for mobile fuel cell applications since it has low boiling temperature (65°C). Therefore, it can be stored in a liquid state at atmospheric pressure and normal environment temperature, unlike liquefied methane (-163°C) [32,33]. In addition, as no carbon–carbon bond exists, methanol can be converted to hydrogen at lower temperature (150~350°C) than other carbon-based fuels, and it can be activated at lower temperature than methane [32]. With these advantages, methanol steam reforming has been widely developed. Faungnawakij et al. has investigated the effect of varying S/C ratio (0~10), reforming temperatures

(25~1000°C), and pressures (0.5−3 atm) on the steam methanol reforming process. Results show that the optimized operating condition based on efficiency was the temperature range of 100~225°C, S/C range of 1.5~3, and pressure at 1 atm. In addition, an operating temperature higher than approximately 150°C and operating pressure varying from 0.5 to 3 atm did not affect the methanol conversion and hydrogen yield [24]. Herdem et al. modeled the methanol steam reforming system to produce power using a HT-PEMFC for portable power generation and examined performance variation of the HT-PEMFC with varying composition of reformate gas. The result reveals that lower S/C ratio and higher reforming temperature increase CO mole fraction in the reformed gas. However, higher fuel cell temperatures decrease the effect of CO mole fraction on the HT-PEMFC performance. [32]. Mousavi Ehteshami and Chan analyzed the steam reforming of methanol, ethanol, and diesel in a technical and economical point of view. It was found that steam methanol reforming showed the easy conversion and the highest energy efficiency. Therefore, methanol is considered to be one of the promising fuels for hydrogen production by using steam reforming. However, the model used in the study did not take into account heat recovery and heat integration in the system. Therefore, it is possible that the efficiencies of fuels with higher reforming temperature than methanol can be increased when heat recovery and integration are applied [34]. Romero-Pascual and Soler investigated an HT-PEMFC-based CHP system integrated with a methanol steam reformer. The result reveals that 24% of system power efficiency and a CHP efficiency over 87% were achieved [12].

Table. 3 Simulation parameters about steam methane and steam methanol reforming from the open literature.

Ref.	Primary Fuels	S/C Ratio	P_{ref} (Bar)	T_{ref} (°C)	Notes
[28]	Methane	3.2	10	700	Purpose of paper was to evaluate performance of hydrogen production via steam methane reforming.
[35]		4	25	900	Steam methane reforming system was modeled and reformer in simulation was developed using a Gibbs equilibrium model in Aspen Plus. For CO_2 capture, MEA scrubbing process was applied as black box model.
[36]		3	1	700	Steam methane reforming system integrated with HT-PEMFC was simulated and performance was evaluated by exergy analysis.
[37]	Methanol	1.2	–	350	Steam methanol reforming system integrated with PEMFC was simulated and performance was evaluated by exergy analysis.
[38]		1.5	3.8	260	Steam methanol reforming system was experimented and the obtained results were used for simulation of power train integrated system.
[39]		1–2	–	240–300	Steam methanol reforming system integrated with HT-PEMFC was simulated. Parametric study with varying S/C ratio, Tref, reformate composition, etc. were implemented.

Chapter 4 System Descriptions

4.1 Reference Ship Description

A general cargo ship with main engine power of 3800kW is chosen as the reference ship for integrating the steam reforming, HT-PEMFC systems. Although the operational engine load depends on the ship design, in general, it can be much smaller than the engine total capacity [40]. Therefore, in this study, the systems are designed based on the average shaft power. This approach allows a more detailed evaluation of the amount of fuel consumption. To calculate the average shaft power, a load factor that indicates the fraction of power needed by the engine to navigate at the average speed was calculated by using the average and maximum speeds. The product of load factor and total installed engine power (MCR) provides the average shaft power [41]. The formulas for load factor and average shaft power are presented in the equations below. The detailed specifications of the reference ship, including the calculated load factor and average shaft power, are presented in Table 4.

$$Load\ Factor = \left(\frac{Average\ Speed}{Max\ Speed}\right)^3 \tag{6}$$

$$Average\ Shaft\ Power[kW] = Load\ Factor \times MCR\ [kW] \tag{7}$$

In the present study, for simplicity of system design, the power required for propulsion excluding other hotel powers are only considered .

Table 4. Specification of the reference ship

Specifications	Values
Type	General Cargo
Overall length	120 m
Beam	13 m
Deadweight	3000 tonnage
Main engine power	3800kW
Maximum speed	14 knots
Average speed	7 knots
Total voyage time	209 h
Load factor	0.125
Average shaft power	475kW

4.2 Description of Steam Methane Reforming-Based System

Figure 10 shows the block diagram of the steam methane reforming system combined with HT-PEMFC on board ships. The integrated system consists of four main unit: Reformer for producing reformate gas, combustor for providing heat to reformer, WGS reactor for conversion of CO to CO_2, HT-PEMFC for power generation.

Natural gas is normally used as feedstock for steam methane reforming and it normally contains small amounts of sulfur compounds, which must be removed to avoid contamination of the catalyst in the reformer and low temperature shift reactor [42]. However, in the proposed system, LNG was considered as feedstock for reforming. As an industry practice, prior to liquefaction, natural gas is further treated to remove sulfur compounds along with water and any residual CO_2 to avoid freezing [43]. Therefore, a desulfurization unit was not included in this study.

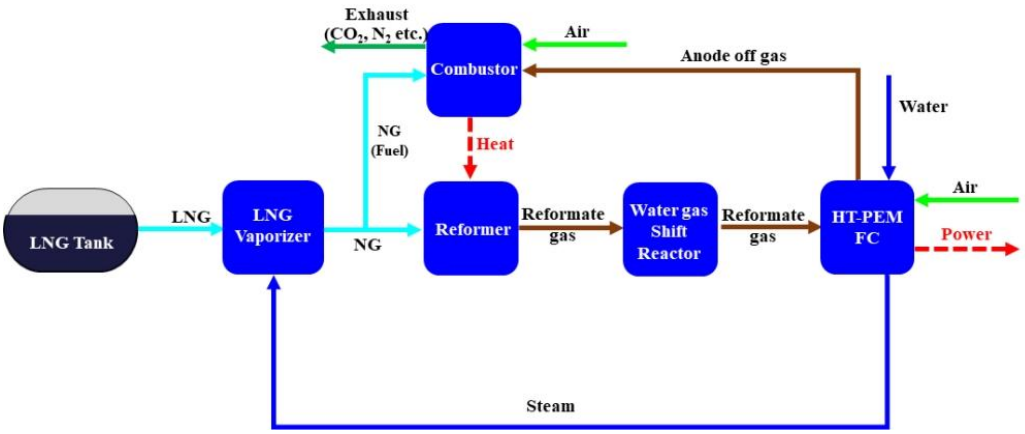

Fig. 10 Block diagram of steam methane reforming-based system

As shown in Figure 11, liquefied from an on-board storage tank is pumped and vaporized by heat exchange with the captured CO_2 in HEX-1. Then, the vaporized CH_4 is divided into two streams: One as feedstock for reforming (stream F4), the other as fuel for the combustor (stream F7). The CH_4 used as feedstock is mixed with high temperature steam (stream W3) and further preheated by heat exchange with the reformate gas stream from the reformer at HEX-2. Then, the steam methane mixture (stream F6) is supplied to the reformer, where the reforming reaction occurs as expressed in Equations (8) and (9), and converted to H_2, CO, and CO_2. The steam methane reforming reaction is highly endothermic; therefore, a large amount of heat must be supplied by the combustor by burning supplemental methane as fuel and by burning off-gas (mostly unreacted CH_4 and unused H_2) from the fuel cell. The operating temperature and pressure for the steam methane reformer in this model were set as 700°C and 3 bar, respectively. The steam to carbon molar ratio (S/C) of 3:1 was applied to avoid coke formation.

$$CH_4 + H_2O = CO + 3H_2 \qquad \triangle H_{298} = 206.3\ kJ\ mol^{-1} \qquad (8)$$

$$CH_4 + 2H_2O = CO_2 + 4H_2 \qquad \triangle H_{298} = 165\ kJ\ mol^{-1} \qquad (9)$$

The reformate gas exiting HEX-2 (stream R2) is further used to preheat air entering to the combustor, and then enters the WGS reactor. The WGS reaction is moderately exothermic and it converts undesired CO in reformate gas to CO_2 and H_2, as shown in Equation (10). The WGS reactor is modeled as a single stage, and the reaction occurs at 250°C. The heat produced during the WGS reaction is used for steam generation.

$$CO + H_2O = CO_2 + H_2 \qquad \triangle H_{298} = -41\ kJ\ mol^{-1} \qquad (10)$$

The reformate gas leaving the WGS rector (stream R4), which has an acceptable level of CO content (< 1%) for the HT-PEMFC, is firstly cooled down to 160°C and then supplied to the anode side of the HT-PEMFC. Dry air is supplied to the cathode side and used for the fuel cell reaction, converting the chemical energy of hydrogen to electricity. Unreacted hydrogen is supplied to the combustor for heat generation. The exhaust gas from the combustor preheats the water supplied to the reformer.

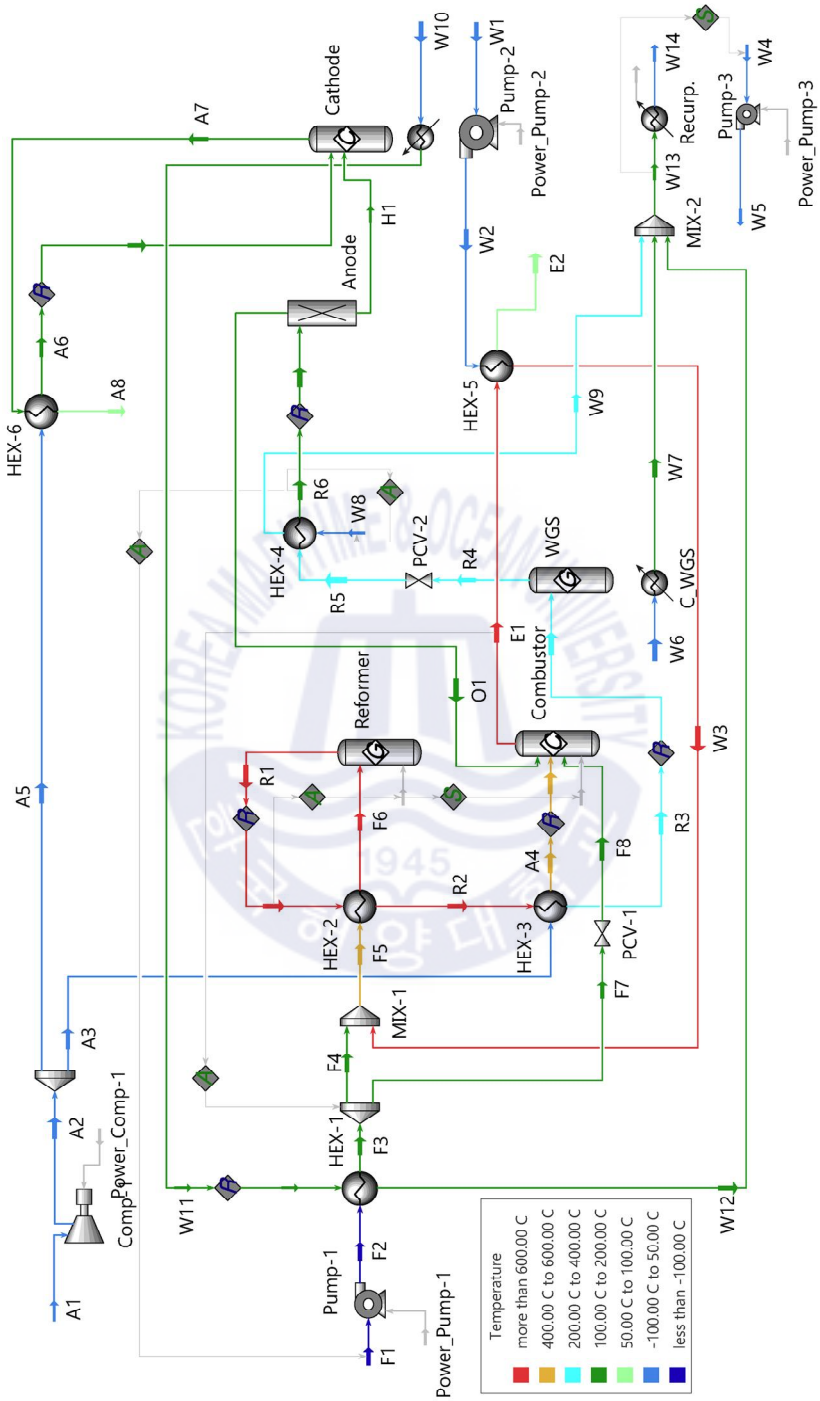

Fig. 11 Process flow diagram for steam methane reforming-based system

4.3 Description of Steam Methanol Reforming-Based System

Figure 12 shows the block diagram of the steam methanol reforming system combined with HT-PEMFC on board a ship. The integrated system consists of three main units: Reformer for producing reformate gas, combustor for providing heat to the reformer, HT-PEMFC for power generation. Unlike the steam methane reforming system, the WGS reactor is not added because the hydrogen rich gas produced in steam methanol reforming includes CO contents tolerable to the HT-PEMFC in this study.

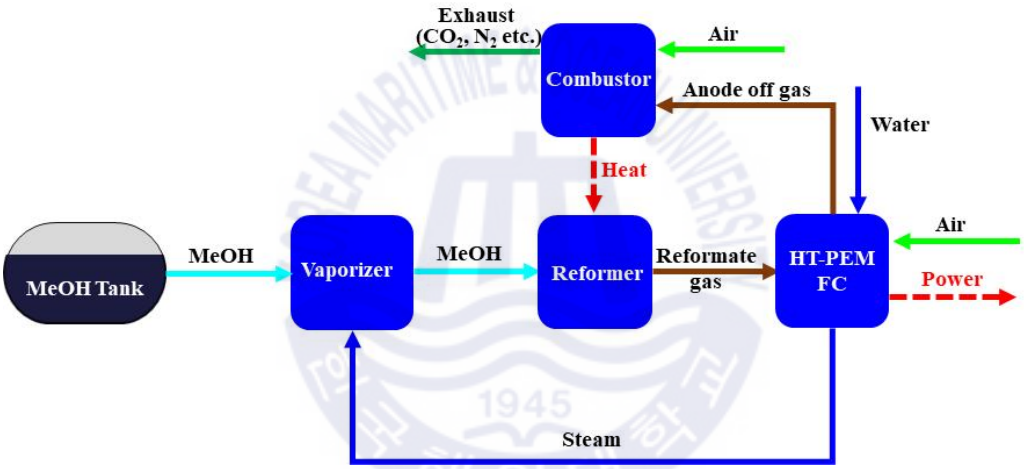

Fig. 12 Block diagram of steam methanol reforming-based system

As shown in Figure 13, methanol and water are mixed at 25°C. The water and methanol mixture is preheated by the steam generated at the HT-PEMFC at HEX-1 and further vaporized by the reformate gas stream (stream R1) from the reformer at HEX-2. Then, H_2 rich reformate gas is produced in the reformer. The main reactions that take place in the reformer are as follows [44]:

$$CH_3OH + H_2O = CO_2 + 3H_2 \qquad \triangle H_{298} = 49.7\ kJ\ mol^{-1} \qquad (11)$$

$$CO + H_2O = CO_2 + H_2 \qquad \triangle H_{298} = -41\ kJ\ mol^{-1} \qquad (12)$$

$$CH_3OH = CO + 2H_2 \qquad \triangle H_{298} = 90.7\ kJ\ mol^{-1} \qquad (13)$$

Equation (11) represents the steam methanol reforming reaction, Equation (12) represents the water gas shift reaction, and Equation (13) represents the methanol decomposition reaction. Only the WGS reaction is exothermic and the other two are endothermic. The operating temperature and pressure for the steam methanol reformer in this model are 200°C and 3 bar, respectively. A S/C ratio of 1.5:1 was selected based on literature reviews [32,38]. Reformate gases containing H_2, CO_2, CO, and CH_3OH exiting HEX-2 are further adjusted to 160°C at HEX-3 and 1.1 bar by PCV-1. Then, the reformate gas is fed to the anode side of the HT-PEMFC for power generation. As off-gas (stream O1) from the fuel cell contains H_2 unreacted in the fuel cell and CH_3OH unconverted in the reformer, the fraction of these is supplied to the combustor to produce heat. The remaining is recycled to the anode inlet stream. The exhaust gas stream (E1) from the combustor preheat air is supplied to the combustor, and the remaining heat in the exhaust gas is recovered in HEX-5. The operating and design parameters of the steam methane and methanol reforming system combined with HT-PEMFC systems are presented in Table 5.

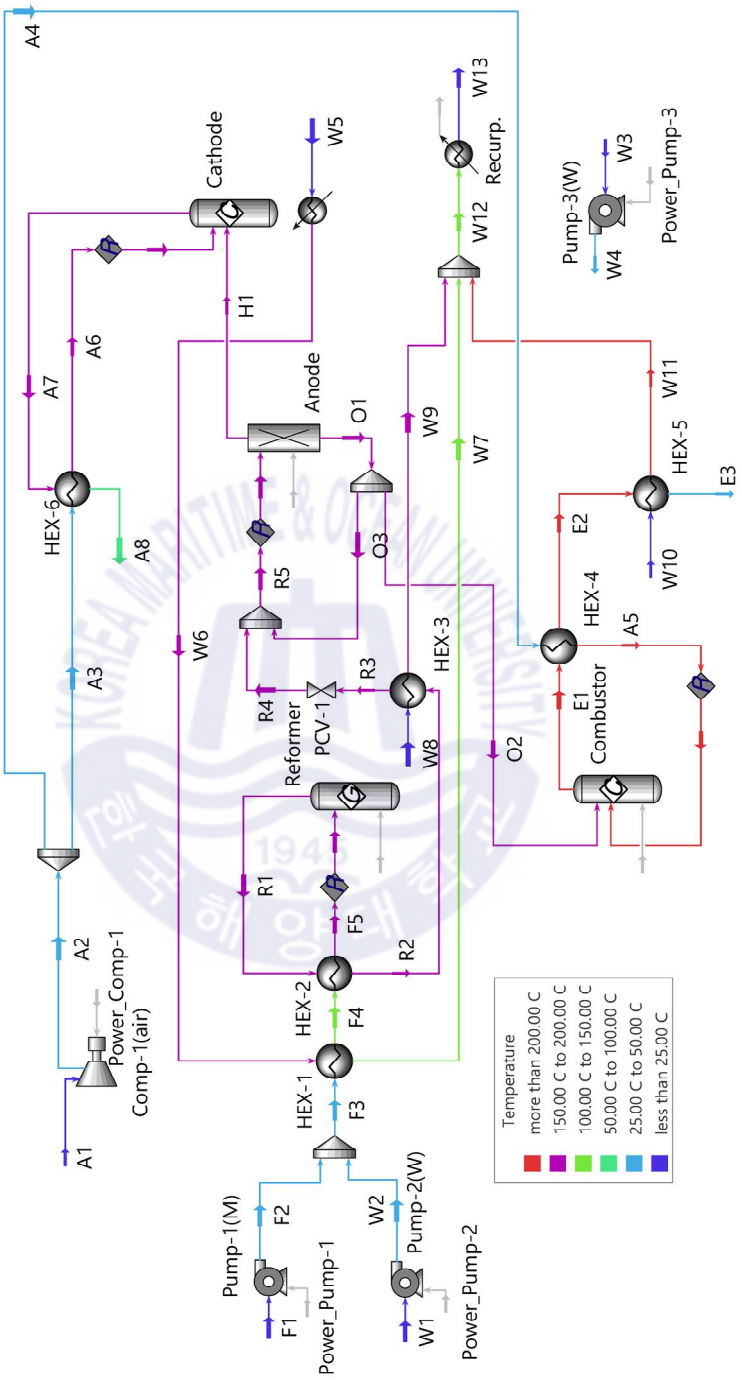

Fig. 13 Process flow diagram for steam methanol reforming-based system

Table 5. Base condition of simulations.

Unit Name	Parameter	Values	
		Steam Methane Reforming-Based System	Steam Methanol Reforming-Based System
Steam reformer	Operating temperature	700°C [36,28]	200°C [39]
	Operating pressure	3 bar	3 bar
	S/C ratio	3 [36,45]	1.5 [32]
WGS reactor	Operating temperature	250°C [46]	–
	Operating pressure	1.1 bar	–
Combustor	Operating temperature	800°C	300°C
	Operating pressure	1.1 bar	1.1 bar
	Air-fuel ratio	1.05 [4]	1.05 [32]
HT-PEMFC	Fuel utilization factor	0.83 [36,47]	
	Cathode stoichiometric ratio	2 [36,47]	
	Operating temperature	160°C [36]	
	Operating pressure	1.1 bar	
	Output voltage per cell	0.637V [48]	
	Current density	0.2 A cm^{-2} [48]	
Compressors	Polytropic efficiency	75%	
Pump	Adiabatic efficiency	85%	
Converter	Efficiency	98% [49]	
Heat exchangers	Min. temperature approach	10°C	
Net electrical power (AC)		475 (±0.2)kW	

Chapter 5 System Simulation and Assumptions

The process simulation and heat and mass balance calculations were carried out using the ASPEN HYSYS process simulator. The heat and mass balances obtained from the converged simulation are utilized for exergy and energy calculations in a separate spreadsheet. The Peng–Robinson equation of state is used for different units/sub-systems including steam reforming, HT-PEMFC system [50]. A "Gibbs reactor" model, which considers the condition of the Gibbs free energy of the reacting system being at a minimum at equilibrium to calculate the product mixture composition [51], is used to simulate the reformer and WGS reactor, whereas the "conversion reactor" model is used to simulate the combustor [42]. There is no separate module to simulate a fuel cell in ASPEN HYSYS. Therefore, in the present study, the HT-PEMFC is modeled as a "conversion reactor" and a "splitter," which attain a conversion ratio equal to the hydrogen utilization factor [11,12].

The concentration of H_2, CO_2, and CO in the anode inlet stream can affect performance of HT-PEMFC. Andreasen et al. investigated the variation of HT-PEMFC performance by the feeding mixture of H_2, CO (0%, 0.15%, 0.25%, 0.5%, 1%), CO_2 (0%, 25%) to emulate methanol or methane reformate gas. Results reveal that increasing both CO and CO_2 concentration decreases output voltage. In total, eight cases of experiments, 1% CO and 25% CO_2 case and 0.5% CO and 25% CO_2 case show the first and second lowest output voltage, approximately 0.645 and 0.652 V, respectively, at 0.2 Acm^{-2} and operating temperature of 160°C [52]. Other experimental studies show similar results. Devrim et al. evaluated the combined effect of CO and CO_2 in anode inlet stream and results show that no significant performance degrade due to the addition of only CO_2 into H_2, however addition of CO in H_2 and CO_2 mixture increase degrade of performance. H_2, CO_2, CO (75%, 24%, 3% and 75%, 24%, 1%) mixtures show output voltage of

approximately 0.629 and 0.634V at 0.2 Acm^{-2} and operating temperature of 160°C [53]. It was reported that the impact of the CO presence (up to 2.0%) at higher operating temperature (160°C and above) and lower current densities (below 0.3 Acm^{-2}) is very low [54,55]. Therefore, in this study, the performance degrade due to CO contents is neglected and output voltage of HT-PEMFC is fixed as 0.637 V [48]. The following I-V curve is used in this study.

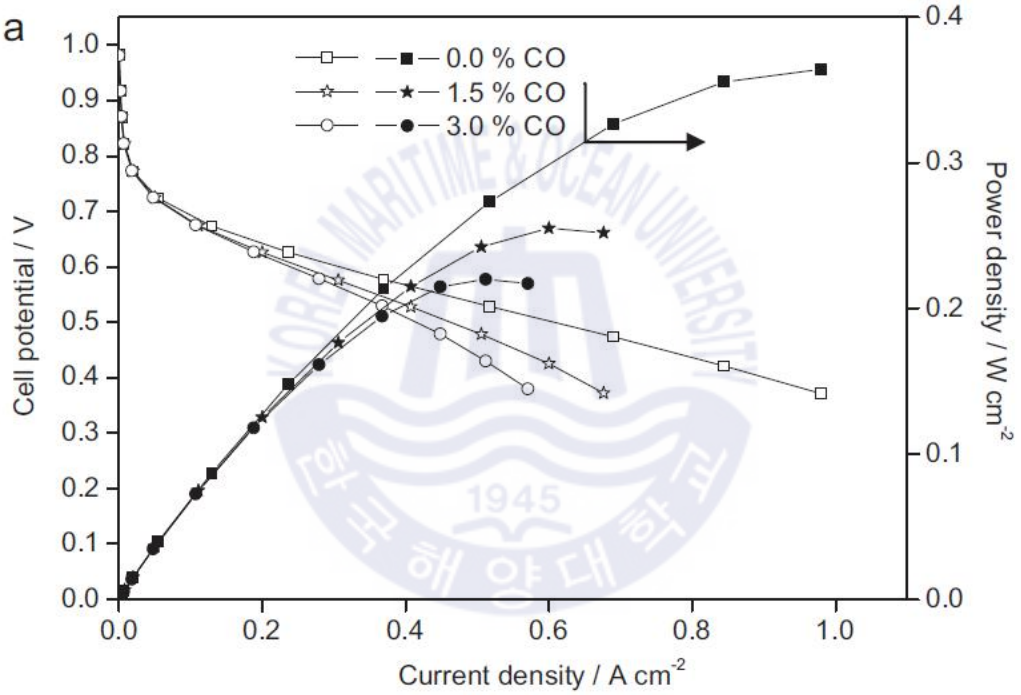

Fig. 14 Polarization and power density curves at 160℃ for three different anode fuels: 0.0% of CO, 1.5% of CO and 3.0% of CO. [48]

Since the amount of electricity consumption vary with several operation modes of ship, it is assumed that the target ship operates with constant average shaft power, namely 475kW for simplicity. Further, a current density of 0.2 Acm^{-2} is assumed for constant power generation. Noteworthy, lower current densities lead to higher

electrical efficiency, and require a larger cell area. However, considering the feasibility check and comparison for ship application of the methane-, methanol-based system is main purpose of this study, the above assumptions are deemed reasonable.

The general assumptions used in the modeling of the integrated energy system are as follows:

- The simulations are implemented in a steady state and are not suitable for start-up operations.
- The composition of air is considered to be 79% N_2 and 21% O_2 on a mole basis.
- For simplicity, LNG is represented by pure, liquefied CH_4.
- The reaction time is considered long enough to achieve phase and chemical equilibrium.
- The reformate gases exiting the reformer are at the reformer temperature.
- Heat and pressure losses are assumed to be negligible in all operational units.
- Complete fuel oxidation is assumed in the combustor.
- The heat ejected from coolers is not recovered.

Chapter 6 Methodology for Performance Evaluation

To conduct a comparative analysis between the steam methane reforming-based system and the steam methanol reforming-based system, energy, exergy efficiency, and exergy destruction rate are used along with fuel cost and fuel storage volumes.

6.1 Energy Analysis of the Integrated Systems

The objective functions that are used in the energy analysis for system performance evaluation are electrical efficiency ($\eta_{en,sys,electrical}$) and cogeneration efficiency (η_{cogen}). The electrical efficiency of the systems is defined as the ratio of the net electrical power output of the system to the lower heating value of the feed and fuel entering the system, as expressed in Equation (14) for the steam methane reforming-based system and in Equation (15) for the steam methanol reforming-based system [32,46].

$$\eta_{en,electrical} = \frac{P_{net,electrical}}{(\dot{n}_{feed,CH4} + \dot{n}_{fuel,CH4} \cdot \quad LHV_{CH4})} \tag{14}$$

where LHV_{CH4} is the lower heating value of CH_4. The net electrical power ($P_{net,electrical}$) is calculated by subtracting the power consumed in the system (P_{pump-1} + P_{pump-2} + P_{pump-3} + P_{comp-1} + P_{comp-2} + P_{comp-3}) from the power generated in the HT-PEMFC ($P_{HT\text{-}PEMFC,AC}$).

$$\eta_{en,electrical} = \frac{P_{net,electrical}}{(\dot{n}_{feed,CH3OH} + \dot{n}_{fuel,CH3OH} \cdot \quad LHV_{CH3OH})} \tag{15}$$

The electrical power generated by HT-PEMFC ($P_{HT\text{-}PEMFC,AC}$) can be calculated as follows [56]:

$$P_{HT-PEMFC} = \eta_{HT-PEMFC} \cdot \quad n_{H2} \cdot \quad LHV_{H2} \cdot \quad \eta_{Converter} \tag{16}$$

where is the molar flow rate of hydrogen that reacts in the HT-PEMFC, LHV_{H2} is the lower heating value of hydrogen, $\eta_{HT\text{-}PEMFC}$ is the electrical efficiency of the HT-PEMFC, and $\eta_{Converter}$ is the efficiency of the converter.

The efficiency of HT-PEMFC ($\eta_{HT\text{-}PEMFC}$) can be found from [56]

$$\eta_{HT-PEMFC} = \mu_f \cdot \quad \frac{V_c}{EMF_{\max}} \cdot \quad 100 \tag{17}$$

where μ_f is the fuel utilization factor, V_c is the produced voltage of the cell, and EMF_{max} is the electromotive force when all the energy from the hydrogen fuel cell, the heating value or enthalpy of formation, was converted to electrical energy. Fuel utilization factor, μ_f and EMF_{max} can be determined as follows:

$$\mu_f = \frac{H_{2,consumed}}{H_{2,^{plied}}} \tag{18}$$

$$EMF_{\max} = -\frac{\triangle h_f}{2F} \tag{19}$$

The heat produced in the fuel cell stack can be determined from [57]

$$\dot{Q}_{heat,HT-PEMFC} = \sum(h_{in,c} \cdot \quad \dot{n}_{in,c}) - \sum(h_{out,c} \cdot \quad \dot{n}_{out,c}) + \sum(h_{in,a} \cdot \quad \dot{n}_{in,a}) - \sum(h_{out,a} \cdot \quad \dot{n}_{out,a}) - P_{HT-PEMFC,DC} \tag{20}$$

The cogeneration efficiency of the system ($\eta_{en,sys,cogen}$) is defined as the ratio between the summation of the rate of available heat output and the net electrical power to the lower heating value of the fuel and feed entering the system, as expressed in Equation (21) for the steam methane reforming-based system and in Equation (22) for the steam methanol reforming-based system [46].

$$\eta_{en,\,CH4,\,cogen} = \frac{P_{net,\,electrical} + Q_{net}}{(\dot{n}_{CH4,feed} + \dot{n}_{CH4,fuel} \cdot \quad LHV_{CH4})} \tag{21}$$

$$\eta_{en,\,CH3OH,\,cogen} = \frac{P_{net,\,electrical} + Q_{net}}{(\dot{n}_{CH3OH,feed} \cdot \quad LHV_{CH3OH})} \tag{22}$$

where

$$Q_{net} = Q_{hot\,water\,(W13)} - Q_{water\,(W3)} \tag{23}$$

6.2 Exergy Analysis of the Integrated Systems

Exergy is defined as the maximum amount of useful energy that can be obtained from a stream when it reaches an equilibrium condition with the reference environment while interacting only with this environment [58]. The exergy analysis is applied to measure the exergy destruction and exergy efficiency for each component of the system proposed in this study. The equation of exergy destruction for each component can be derived from the equation of exergy balance. Considering a control volume at steady state, the general form of exergy balance can be written as follows:

$$\sum \dot{E}x_Q - \sum \dot{E}x_W + \sum \dot{E}x_{flow,in} - \sum \dot{E}x_{flow,out} - \sum \dot{E}x_{dest} = 0 \tag{24}$$

where Ex_Q represents the rate of exergy transfer due to heat exchange with the environment, Ex_W is the rate of exergy transfer related to work, Ex_{Dest} represents exergy destruction, and Ex_{flow} corresponds to the exergy transfer rate associated with the flow of the stream.

The total exergy related with the i^{th} stream represents the sum of the physical and chemical exergies as follows [59] :

$$\dot{E}x = \dot{E}x_{ph} + \dot{E}x_{ch} = \dot{m} \cdot (ex_{ph} + ex_{ch}) \tag{25}$$

The specific physical exergy is defined as follows [59] :

$$ex_{ph,i} = h_i - h_0 - T_0(s_i - s_0) \tag{26}$$

Here e, h and s correspond to the specific exergy, enthanpy and entropy of each flow. Subscript 0 refers to the reference conditions. The reference conditions, T_0 and P_0, are set to 25°C and 101.325 kPa in this work.

The specific chemical exergy can be calculated from [59] :

$$ex_{ch,i} = \sum x_l \cdot \quad ex_{ch,l}^{std} + RT_0 \sum x_l \cdot \quad \ln x_l \tag{27}$$

$ex_{ch,i}^{std}$ is the standard molar chemical exergy of the substance l. x_l denotes the mole fraction of substance l in the stream i.

The equations for the exergy destruction of each component are summarized in Table 6.

Table. 6 Equation of exergy destruction and efficiency of the components

Components	Exergy Destruction
Compressors [45]	$\dot{E}x_{dest} = \dot{E}x_{in} + P_{in,comp} - \dot{E}x_{out}$
Pumps [45]	$\dot{E}x_{dest} = \dot{E}x_{in} + P_{in,pump} - \dot{E}x_{out}$
Heat exchangers [45]	$\dot{E}x_{dest} = \dot{E}x_{in} + \dot{E}x_{out})_{hot} + \dot{E}x_{in} + \dot{E}x_{out})_{cold}$
Reformer-Combustor [45]	$\dot{E}x_{dest} = \dot{E}x_{in,feed} + \dot{E}x_{in,fuel} + \dot{E}x_{in,off\ gas} - \dot{E}x_{out,reformate\ gas} - \dot{E}x_{out,exhaust gas}$
WGS [45]	$\dot{E}x_{dest} = \dot{E}x_{in,reformate\ gas} + \dot{E}x_{in,cooling\ water} - \dot{E}x_{out,reformate\ gas} - \dot{E}x_{out,cooling water}$
HT-PEM fuel cell [60,61]	$\dot{E}x_{dest} = \dot{E}x_{in,reformate\ gas} + \dot{E}x_{in,air} + \dot{E}x_{in,cooling\ water} - \dot{E}x_{out,air} - \dot{E}x_{out,cooling water} - \dot{E}x_{out,off\ gas} - P_{out,electrical}$
Coolers	$\dot{E}x_{dest} = \dot{E}x_{in} - \dot{E}x_{out}$
Valves	$\dot{E}x_{dest} = \dot{E}x_{in} - \dot{E}x_{out}$

Chapter 7 Results and Discussion

7.1 Energy and Exergy Analyses

The steam reforming systems presented in this study are evaluated in terms of energy of the overall systems, and exergy destruction rate of each component. For the energy efficiency, electrical and cogeneration efficiencies are utilized. Electrical efficiency and cogeneration efficiency at the base condition presented in Table 5 for the methane-based and methanol-based systems are compared in Figure 15. Electrical efficiencies of 40.49% for the methane-based system and 49.87% for the methanol-based system are obtained. It can be interpreted that the methanol-based system uses the feed energy input (LHV basis) more efficiently than the methane-based system for 475kW of net electricity generation.

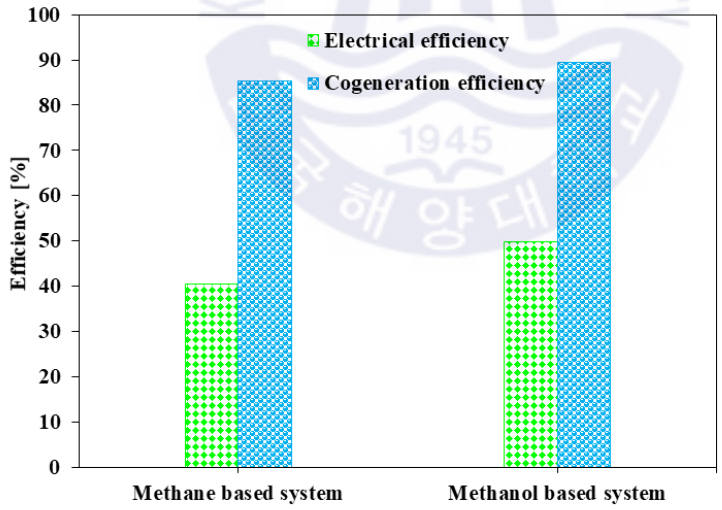

Fig. 15 Electrical and cogeneration efficiencies of the methane-based and methanol-based systems for 475kW of net electricity generation

Noteworthy, the overall electricity consumption of the methane-based and methanol-based systems are 7.41 and 7.13kW, respectively, as indicated in Figure 16. The higher electricity consumption in the methane-based system is mainly attributed to electricity consumption of the air compressors.

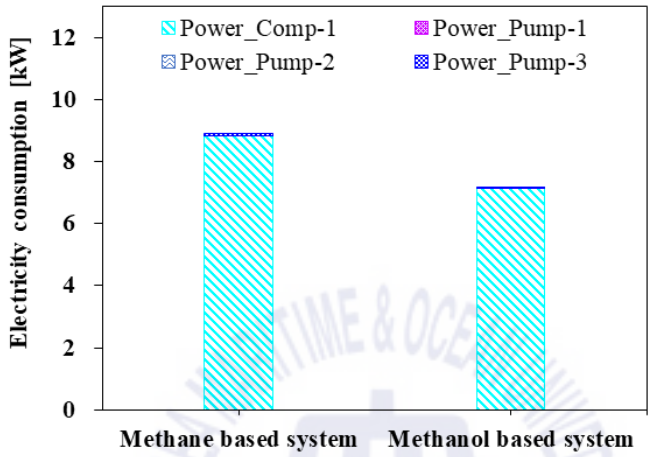

Fig. 16 Break-down of electricity consumption of the methane-based and methanol-based systems for 475kW of net electricity generation.

Regarding the cogeneration efficiency, the methane-based system has higher value, 85.30%, than that of the methanol-based system, 89.53%, and this can be explained by Figure 17. As can be observed in Figure 17, the methane-based system consumes a higher amount of overall energy (LHV basis) than the methane-based system and generates more available heat for 475kW of net electricity generation. The higher value of heat generated can be explained by the fact that the steam methane reforming reaction is more endothermic than the steam methanol reforming reaction.

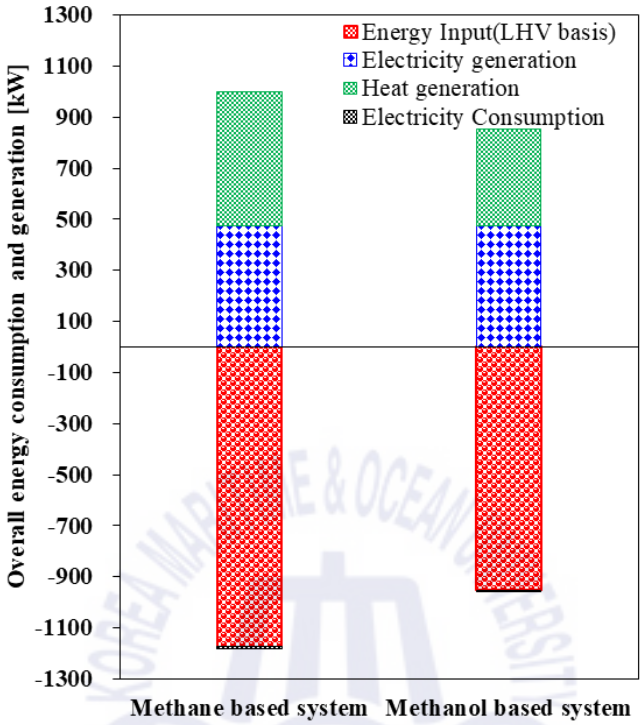

Fig. 17 Overall energy consumption and generation of the methane-based and methanol-based systems for 475kW of net electricity generation.

To evaluate the performance of the components, the exergy destructions of each component in the methane-based and methanol-based systems at the base condition provided in Table 5 are calculated. It is observed that there is a total exergy destruction of 637.24kW for the methane-based system and 481.42kW for the methanol-based system as can be seen in Figure 18. The exergy destructions in each system are broken down to the component level and the results are presented in Figures 19 and 20. The HT-PEMFC, reformer-combustor have the largest percentages of total exergy destruction for both cases. For the methane-based system, the HT-PEMFC is the component having the highest exergy destruction with 336.89kW (52.87%), followed by the reformer-combustor with 155.19kW

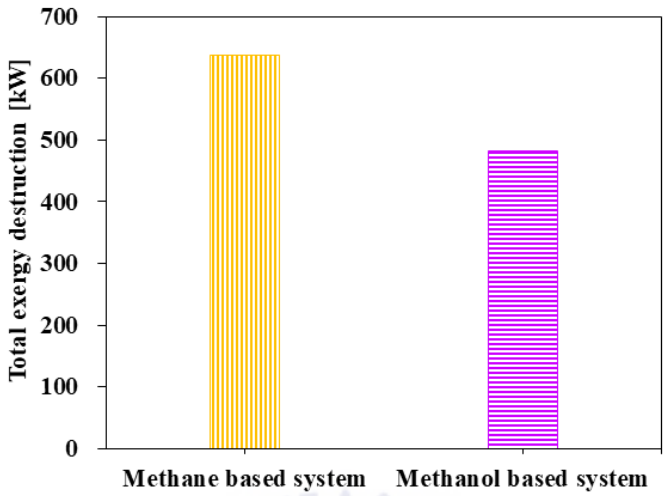

Fig. 18 Total exergy destruction of the methane-based and methanol-based systems for 475 kW of net electricity generation.

(24.35%). The exergy destructions in the methanol-based system follow a similar trend, having the highest exergy destruction in the HT-PEMFC with 321.31kW (66.75%), reformer-combustor with 123.21kW (25.59%). Exergy destruction of the HT-PEMFC and reformer-combustor mainly results from high irreversibility of the chemical reaction [54]. The larger total exergy destruction in the methane-based system is mainly attributed to the larger exergy destruction in the reformer-combustor. This relies on the fact that the steam methane reforming reaction is operated at a higher temperature condition of 700°C (combustion temperature of 800°C) instead of 200°C (combustion temperature of 300°C) in the steam methanol reforming reaction.The other reasons explaining why the total exergy destruction is higher in methane-based systems than in methanol-based systems is that higher exergy destruction occurs in the heat exchangers (mainly HEX-1, HEX-3, and HEX-5), Mixer-1. For the heat exchangers, the larger exergy destruction derives from the larger temperature difference between cold and hot

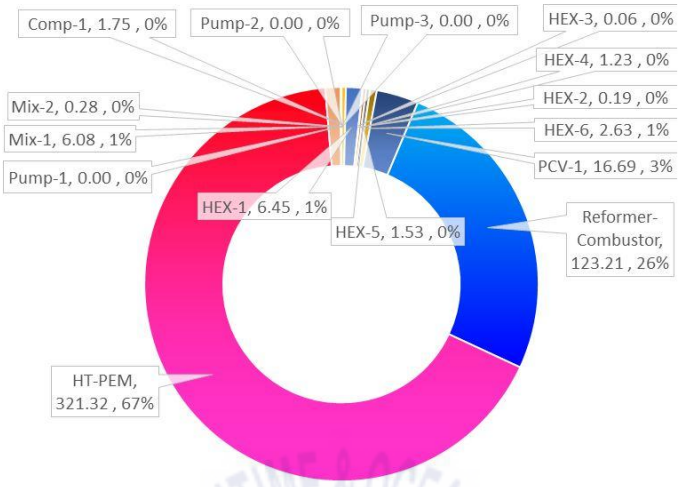

Fig. 19 Break-down of exergy destruction for the methanol based-system. Total exergy destruction 591.16kW. (Unit names: Exergy destruction, kW; exergy destruction ratio, %).

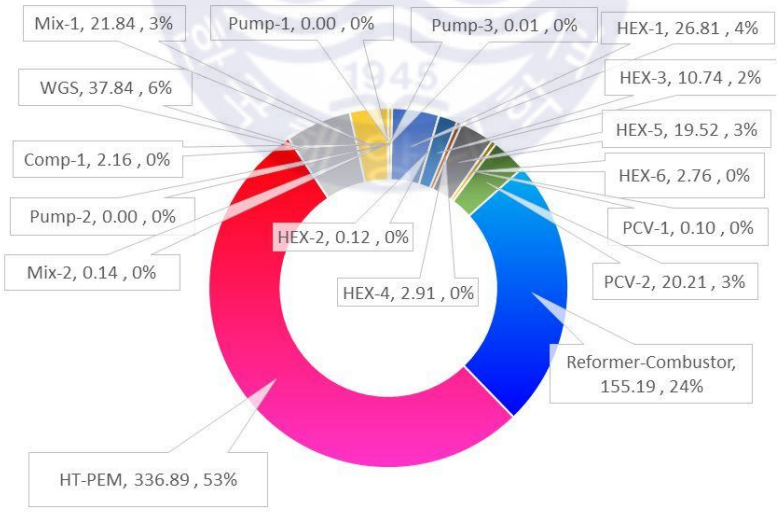

Fig. 20 Break-down of exergy destruction for the methane based-system. Total exergy destruction 690.68kW. (Unit names: Exergy destruction, kW; exergy destruction ratio, %).

streams. This is because fuel in cryogenic temperature (LNG) is supplied in the methane-based system and streams from the reformer and combustor have inherent temperature. For Mix-1, more exergy destruction in the methane-based system than that in the methanol-based system is generated from mixing of streams with larger temperature difference. Therefore, reducing the temperature differences in these heat exchangers and Mix-1 by optimization can effectively reduce the system exergy destruction [71]. The exergy destruction generated in the WGS reactor, which is additionally equipped for the methane-based system to lower the CO fraction, is another reason.

7.1.1 Effect of Varying Reforming Temperature

The variation of H_2 molar flow rate at the outlet of the steam methane and steam methanol reformers in thermodynamic equilibrium with varying reforming temperature and S/C ratio was derived to understand the system behavior. As can be observed in Figures 21, the methane steam reformer shows the tendency that at S/C ratios below 3.5, the hydrogen flow rate increases when the reforming temperature increases up to 750°C. After then, the H_2 molar flow rate decreases as the reforming temperature increases. At S/C ratios above 3.5, the H_2 molar flow rate continuously decreases as the reforming temperature increases. The steam methanol reformer shows a trend that as the reforming temperature increases from 180 to 260°C, the molar flow rate of H_2 continuously decreases, although the decrease rates are different, as shown in Figure 22. Figure 21 and 22 represent the behavior of each reformer and can be used for interpretation of each system in the next section. The effects of varying the reforming temperature on the system efficiencies in the methane-based and methanol-based systems were studied and illustrated in Figure 23 and 24 respectively.

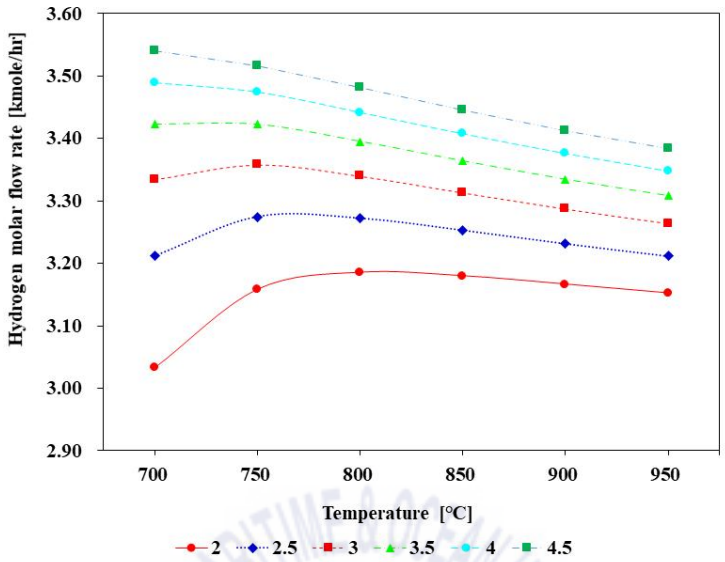

Fig. 21 Variation of H_2 molar flow rates of the exit gases from the reformer as a function of the S/C ratio and reforming temperature - Steam methane reformer : Methane supply of 1 kmole/h

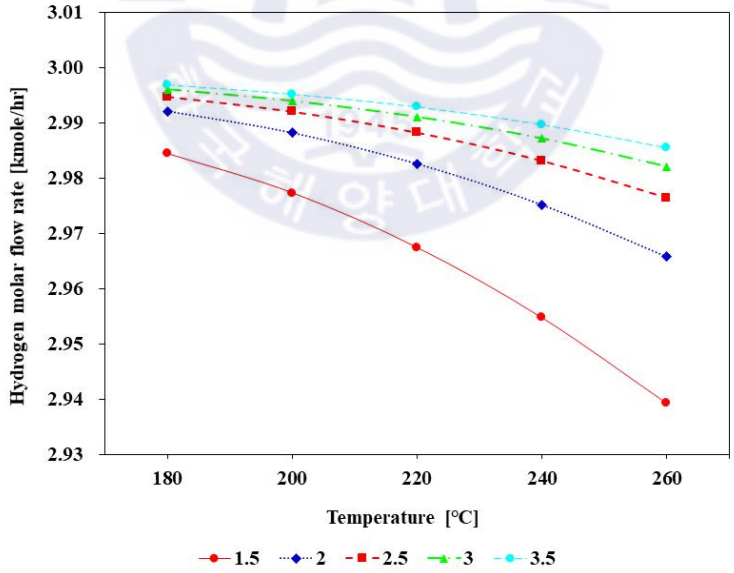

Fig. 22 Variation of H_2 molar flow rates of the exit gases from the reformer as a function of the S/C ratio and reforming temperature - Steam methanol reformer: Methanol supply of 1 kmole/h

As can be observed in Figure 23, for the methane-based system, as the reforming temperature increases from 700 to 950°C, the electrical efficiency continuously decrease from 40.49% to 38.32%. The amount of available heat also decrease from 700 to 950°C. This trend occurs because as the reforming temperature increases, the amount of additional fuel needed for the reformer and combustor increases and leads to a decrease in efficiencies of the system. It can be noticed that the slope of the available heat between 700 and 800°C is more steep than that at other temperature ranges. The reason for this is that the amount of hydrogen produced are relatively higher between 700 to 800°C, as shown in Figure 21.

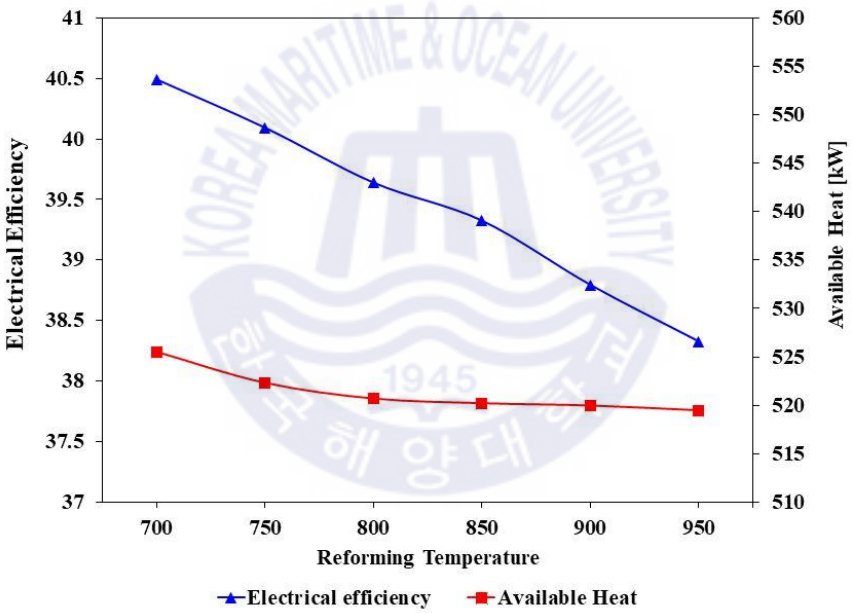

Fig. 23 Influence of reforming temperature on system efficiencies - Methane-based system (S/C ratio: 3)

The methanol-based system shows a similar behavior to that of the methane-based system, as shown in Figure 24. As the reforming temperature increases from 180 to 260°C, the electrical efficiency increase from 50.18% to 48.55%, whereas the amount of the available heat continuously increase unlike the

methane-based system. This happens because temperature for methanol reforming is relatively lower than that of methane reforming reaction.

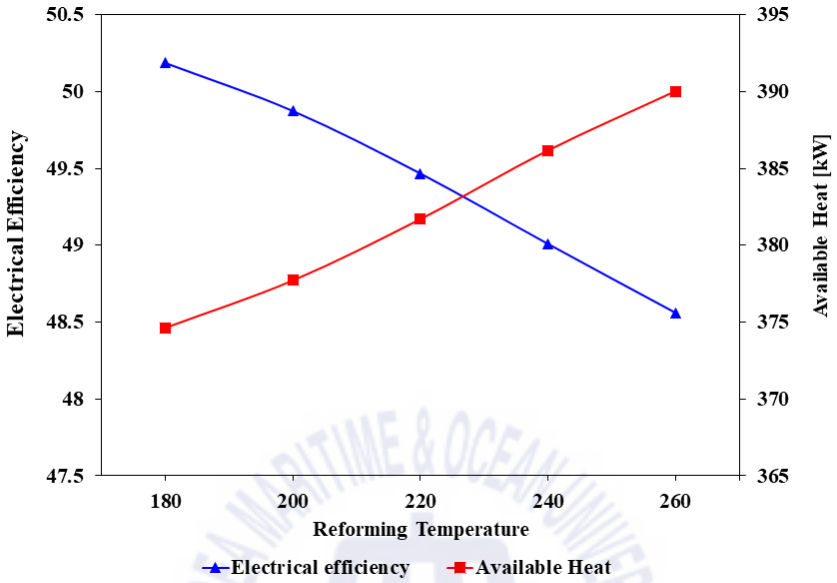

Fig. 24 Influence of reforming temperature on system efficiencies - Methanol-based system (S/C ratio: 1.5)

7.1.2 Effect of Varying Steam to Carbon Ratio

Figure 25 shows the change in the electrical efficiency with varying S/C ratio for the methane-based system. For the steam methane-based system, when the S/C ratio is increased from 2 to 4.5, the electrical efficiency decrease from 41.72% to 39.37%. This tendency occurs because a higher S/C ratio requires a considerable amount of heat to produce steam, resulting in more fuel consumption in the combustor. The increase in parasitic power consumption for the pump and compressor is another reason for the decrease in electrical efficiency. In case of the available for methane-based system also increase with increasing S/C ratio. This is because as S/C ratio increase, more heat is produced in combustor, then unused heat in combustor is recovered.

The methanol-based system shows a similar behavior to that of the

methane-based system, as shown in Figure 26. When the S/C ratio is increased from 1.5 to 3.5, the electrical efficiency decrease from 49.87% to 49.45%.

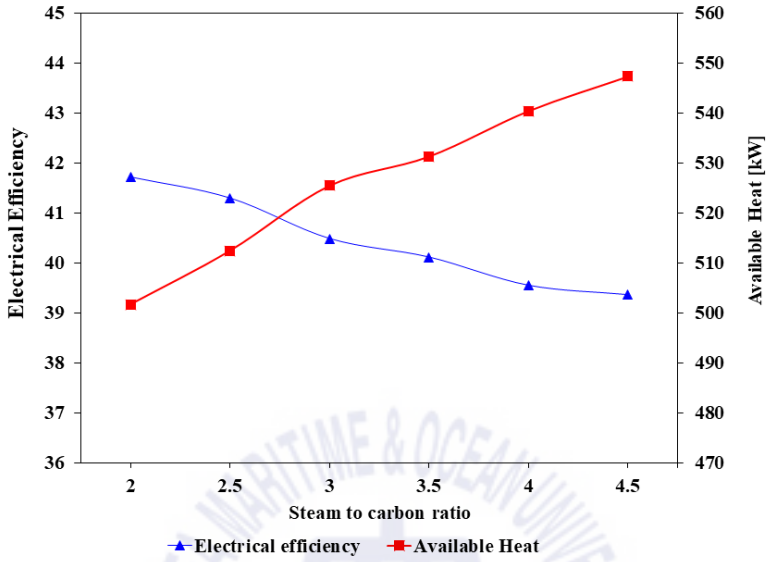

Fig. 25 Influence of S/C ratio on system efficiencies and available heat – methane-based system (reforming temperature: 700°C)

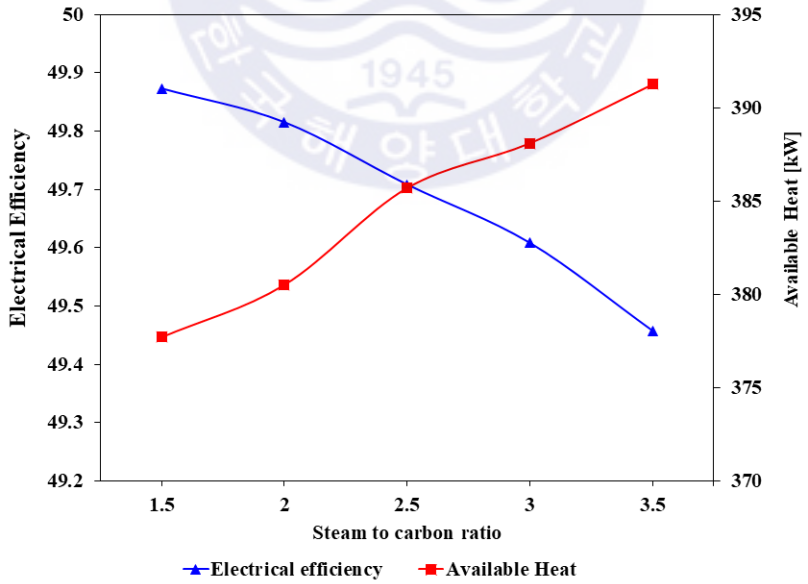

Fig. 26 Influence of S/C ratio on system efficiencies and available heat – methanol-based system (reforming temperature: 200°C)

7.2 Space and Operational Cost

Figure 27 illustrates the volume for storage of the fuel along with the cost of fuels for the methane-based and methanol-based systems, which are required for 475kW of net electricity generation during the total navigation time. A specific fuel cost of 9.76 USD/mmBtu for LNG [62] and 26.08 USD/mmBtu [63] for methanol are used, and both are the average cost in 2018 in the references. The result shows that methane-based system requires 42.65m^3 for LNG storage, whereas the methanol-based system requires 45.77m^3 for methanol. Accordingly, the methanol-based system needs approximately 1.07 times the volume (equivalent to 3.11m^3 more) for fuel storage. In other words, the methanol-based system consumes a more amount of methanol as fuel. Regarding the fuel cost, the methanol-based system has a 2.16 times higher fuel cost than the methane-based system for 475kW of net electricity generation during the total navigation time. Therefore, the methane-based system is more competitive than the methanol-based system from the

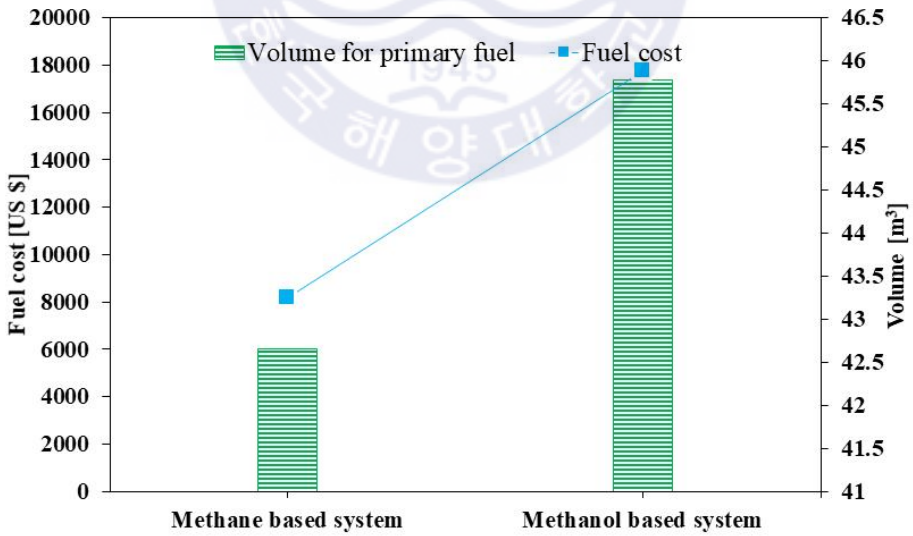

Fig. 27 Fuel volumes and cost of methane-based and methanol-based systems for 475kW of net electricity generation during the total navigation time.

economic point of view, when only the fuel cost and volume are taken into account. However, note that the overall investment cost for both systems, which is beyond the scope of the current study, may also be an important factor in the selection of system.

Chapter 8 Conclusions

In this work, the author have performed a comparison between the steam methane reforming and steam methanol reforming technologies combined with HT-PEMFC and carbon capture systems for hydrogen-fueled ship applications. To find the most suitable technologies, an energy/exergy analysis, along with a space and fuel cost investigation, have been conducted. All the simulations have been conducted at a fixed $W_{net,\ electrical}$ (475kW).

It is shown that, at the base condition, the energy and cogeneration efficiencies of the methanol-based system are 9.37% and 4.23% higher than those of the methane-based system, respectively. The different efficiencies between systems mainly arises from the reforming temperature difference. For fuel storage, the methanol-based system requires a space 1.07 times larger than that of the methane-based system for the total navigation time, although the methanol-based system has higher electrical efficiency. Accordingly, the methanol-based system has 2.16 times higher fuel cost than the methane-based system for 475kW of net electricity generation during the total navigation time. In the parametric study, both systems show a similar trend, in which with increasing reforming temperature and S/C ratio, the electrical efficiency gradually decreased.

The comparative analysis reveals that the methanol-based system has many technological advantages directly related to its low reforming temperature, which leads to better integration to the HT-PEMFC. However, the methane-based system showed economic advantages from the perspective of fuel cost and better availability in the maritime sector.

Several limitations were identified for consideration in the future study. In the present study, constant current density of 0.2 Acm^{-2} was assumed and resulted in a little higher electrical efficiency. More simulations in several current density within

the operating window of HT-PEMFC are required in the future study. In addition, future study should use output voltage with real reformate gas for the detailed assessment. Present study compared two systems in the process simulation level, however, future study should include sizing and on-board arrangement of systems since those systems may take large spaces and lead to different results. Furthermore, other fuels such as ethanol and liquefied petroleum gas (LPG) which is getting attention together with methanol and LNG in maritime industry should be assessed in the future study. Although the present study has some limitations, the concepts suggested in this study can give other perspectives on applying hydrogen fuel cell on board and can be a good reference for the further development of hydrogen fuel cell ship.

Reference

1. International Maritime Organization. Third IMO Greenhouse Gas Study. Available online: http://www.imo.org/en/OurWork/Environment/PollutionPrevention/AirPollution/Pages/Greenhouse-Gas-Studies-2014.aspx (accessed on 30 December 2019).

2. DNV GL. Maritime forecast to 2050, Energy transition outlook 2018. Available online: https://eto.dnvgl.com/2018/#Energy-Transition-Outlook-2018- (accessed on 30 December 2019).

3. Initial IMO Strategy on the Reduction of GHG Emissions From Ships. Resolution MEPC; Available online: http://www.imo.org/en/MediaCentre/HotTopics/GHG/Pages/default.aspx (accessed on 30 December 2019).

4. Zhu, M.; Fai, K.; Wei, J.; Li, K.X. Impact of maritime emissions trading system on fleet deployment and mitigation of CO2 emission. Transp. Res. Part D 2018, 62, 474–488.

5. van Biert, L.; Godjevac, M.; Visser, K.; Aravind, P.V. A review of fuel cell systems for maritime applications. J. Power Sources 2016, 327, 345–364.

6. Balcombe, P.; Brierley, J.; Lewis, C.; Skatvedt, L.; Speirs, J.; Hawkes, A.; Staffell, I. How to decarbonise international shipping: Options for fuels, technologies and policies. Energy Convers. Manag. 2019, 182, 72–88.

7. Tronstad, T.; Astrand, H.H.; Haugom, G.P. Langfeldt, L. Study on the Use of Fuel Cells in Shipping. Available online: http://www.emsa.europa.eu/component/flexicontent/download/4545/2921/23.html (accessed on 30 December 2019).

8. Minnehan, J.J.; Pratt, J.W. Practical Application Limits of Fuel Cells and Batteries for Zero Emission Vessels. 2017.

9. Alvarez, C.; Fern, C.; Carral, L. Analysing the possibilities of using fuel cells in ships. Int. J. Hydrog. Energy 2015, 41, 2853–2866. doi:10.1016/j.ijhydene.2015.11.145.

10. Rr-mp, D.G. Application of Fuel Cells in Surface Ships. 2001.

11. Jaggi, V.; Jayanti, S. A conceptual model of a high-efficiency, stand-alone power unit based on a fuel cell stack with an integrated auto-thermal ethanol reformer. Appl. Energy 2013, 110, 295–303.

12. Romero-Pascual, E.; Soler, J. Modelling of an HTPEM-based micro-combined heat and power fuel cell system with methanol. Int. J. Hydrog. Energy 2014, 39, 4053–4059.

13. Hydrogen Analysis Resource Center. Lower and Higher Heating Values of Fuels. Available online:https://h2tools.org/hyarc/hydrogen-data/lower-and-higher-heating-values-hydrogen-and-other-fuels (accessed on 30 December 2019).

14. Vessels, M. Fuel Cell Applications for Marine Vessels Why Fuel Cells Make Sense. Available online: https://info.ballard.com/fuel-cell-applications-for-marine-vessels (accessed on 30 December 2019).

15. Nerem, T. Assessment of Marine Fuels in a Fuel Cell on a Cruise Vessel. Available oneline: https://ntnuopen.ntnu.no (accessed on 30 December 2019).

16. Sattler, G. Fuel cells going on-board. J. Power Sources 2000, 86, 61–67.

17. Welaya, Y.M.A.; El Gohary, M.M.; Ammar, N.R. Steam and partial oxidation reforming options for hydrogen production from fossil fuels for PEM fuel cells. Alex. Eng. J. 2012, 51, 69–75.

18. e4ships FUEL CELLS IN MARINE APPLICATIONS. Available oneline: https://www.e4ships.de/app/download/13416971890/e4ships_Brochure_engl_2016.pdf?t=1568291372 (accessed on 30 December 2019).

19. Rajasekhar, D.; Narendrakumar, D. Fuel Cell Technology for Propulsion and Power Generation of Ships: Feasibility Study on Ocean Research Vessel Sagarnidhi. J. Shipping Ocean Engineering 2020, 5, 219–228.

20. Saito, N. The Maritime Commons: Digital Repository of the World. The Economic Analysis of Commercial Ships with Hydrogen Fuel Cell through Case Studies. Available oneline: https://commons.wmu.se/cgi/viewcontent.cgi?article=1617&context=all_dissertations (accessed on 30 December 2019).

21. Han, J.; Charpentier, J.F.; Tang, T. State of the Art of Fuel Cells for Ship Applications. In Proceedings of the 2012 IEEE International Symposium on Industrial Electronics, Hangzhou, China, 28 – 31 May 2012.

22. Alvarez, C.; Fern, C.; Carral, L. Analysing the possibilities of using fuel cells in ships. Int. J. Hydrog. Energy 2015, 41, 2853 – 2866. doi:10.1016/j.ijhydene.2015.11.145.

23. Leo, T.J.; Durango, J.A.; Navarro, E. Exergy analysis of PEM fuel cells for marine applications. Energy 2010, 35, 1164 – 1171.

24. Faungnawakij, K.; Kikuchi, R.; Eguchi, K. Thermodynamic evaluation of methanol steam reforming for hydrogen production. J. Power Sources 2006, 161, 87 – 94.

25. ABS, Low Carbon Shipping.

26. Schjolberg, I.; Calo, E.; Van Dijk, E.; Ersoz, A.; Fernandez, E.O.; Hulteberg, C.; Lieftink, D.; Nelsson, C.; Daint-Just, J.; Silversand, F.; et al. IEA-HIA Task 23 Small-scale Reformers for On-site Hydrogen Supply Final report; 2012; ISBN 9780981504148.

27. Chen, B.; Liao, Z.; Wang, J.; Yu, H.; Yang, Y. Exergy analysis and CO2 emission evaluation for steam methane reforming. Int. J. Hydrog. Energy 2012, 37, 3191 – 3200.

28. Simpson, A.P.; Lutz, A.E. Exergy analysis of hydrogen production via steam methane reforming. Int. J. Hydrog. Energy 2007, 32, 4811 – 4820.

29. Alhamdani, Y.A.; Hassim, M.H.; Ng, R.T.L.; Hurme, M. The estimation of fugitive gas emissions from hydrogen production by natural gas steam reforming. Int. J. Hydrog. Energy 2017, 42, 9342 – 9351.

30. Authayanun, S.; Saebea, D.; Patcharavorachot, Y.; Arpornwichanop, A. Effect of different fuel options on performance of high-temperature PEMFC (proton exchange membrane fuel cell) systems. Energy 2014, 68, 989 – 997.

31. Arsalis, A.; Nielsen, M.P.; Kær, S.K. Modeling and parametric study of a 1 kWe HT-PEMFC-based residential micro-CHP system. Int. J. Hydrog. Energy 2011, 36, 5010 – 5020.

32. Herdem, M.S.; Farhad, S.; Hamdullahpur, F. Modeling and parametric study of a methanol reformate gas-fueled HT-PEMFC system for portable power generation applications. Energy Convers. Manag. 2015, 101, 19 – 29.

33. Palo, D.R.; Dagle, R.A.; Holladay, J.D. Methanol steam reforming for hydrogen production. Chem. Rev. 2007, 107, 3992–4021.

34. Mousavi Ehteshami, S.M.; Chan, S.H. Techno-Economic Study of Hydrogen Production via Steam Reforming of Methanol, Ethanol, and Diesel. Energy Technol. Policy 2014, 1, 15–22.

35. Zhu, L.; Li, L.; Fan, J. A modified process for overcoming the drawbacks of conventional steam methane reforming for hydrogen production: Thermodynamic investigation. Chem. Eng. Res. Des. 2015, 104, 792–806.

36. Ye, L.; Jiao, K.; Du, Q.; Yin, Y. Exergy analysis of high-temperature proton exchange membrane fuel cell systems. Int. J. Green Energy 2015, 12, 917–929.

37. Ishihara, A.; Mitsushima, S.; Kamiya, N.; Ota, K.I. Exergy analysis of polymer electrolyte fuel cell systems using methanol. J. Power Sources 2004, 126, 34–40.

38. Wiese, W.; Emonts, B.; Peters, R. Methanol steam reforming in a fuel cell drive system. J. Power Sources 1999, 84, 187–193.

39. Lotrič, A.; Sekavčnik, M.; Pohar, A.; Likozar, B.; Hočevar, S. Conceptual design of an integrated thermally self-sustained methanol steam reformer−High-temperature PEM fuel cell stack manportable power generator. Int. J. Hydrog. Energy 2017, 42, 16700–16713.

40. Berstad, D.; Anantharaman, R.; Nekså, P. Low-temperature CO2 capture technologies−Applications and potential. Int. J. Refrig. 2013, 36, 1403–1416.

41. Minnehan, J.J.; Pratt, J.W. Practical Application Limits of Fuel Cells and Batteries for Zero Emission Vessels. Available online: https://energy.sandia.gov (accessed on 30 December 2019).

42. Hajjaji, N.; Pons, M.N.; Houas, A.; Renaudin, V. Exergy analysis: An efficient tool for understanding and improving hydrogen production via the steam methane reforming process. Energy Policy 2012, 42, 392–399.

43. Liquefied Natural Gas (LNG) Operations Consistent Methodology for Estimating Greenhouse Gas Emissions. Available online: https://www.api.org (accessed on 30 December 2019).

44. Iulianelli, A.; Ribeirinha, P.; Mendes, A.; Basile, A. Methanol steam reforming for hydrogen generation via conventional and membrane reactors: A review. Renew. Sustain. Energy Rev. 2014, 29, 355–368.

45. Tzanetis, K.F.; Martavaltzi, C.S.; Lemonidou, A.A. Comparative exergy analysis of sorption enhanced and conventional methane steam reforming. Int. J. Hydrog Energy 2012, 37, 16308–16320.

46. Nalbant, Y.; Colpan, C.O.; Devrim, Y. Energy and exergy performance assessments of a high temperature-proton exchange membrane fuel cell based integrated cogeneration system. Int. J. Hydrog. Energy 2019, 1–11. doi:10.1016/j.ijhydene.2019.01.252.

47. Ribeirinha, P.; Abdollahzadeh, M.; Sousa, J.M.; Boaventura, M.; Mendes, A. Modelling of a high-temperature polymer electrolyte membrane fuel cell integrated with a methanol steam reformer cell. Appl. Energy 2017, 202, 6–19

48. Boaventura, M.; Sander, H.; Friedrich, K.A.; Mendes, A. The influence of CO on the current density distribution of high temperature polymer electrolyte membrane fuel cells. Electrochimica Acta 2011, 56, 9467–9475.

49. Ersoz, A.; Olgun, H.; Ozdogan, S. Simulation study of a proton exchange membrane (PEM) fuel cell system with autothermal reforming. Energy 2006, 31, 1490–1500.

50. Zohrabian, A.; Mansouri, M.; Soltanieh, M. Techno-economic evaluation of an integrated hydrogen and power co-generation system with CO2 capture. Int. J. Greenh. Gas Control 2016, 44, 94–103.

51. Haydary, J. Chemical Process Design and Simulation: Aspen Plus and Aspen Hysys Applications; John Wiley & Sons: Hoboken, NJ, USA, 2019; ISBN 1119089115.

52. Andreasen, S.J.; Vang, J.R.; Kær, S.K. High temperature PEM fuel cell performance characterisation with CO and CO2 using electrochemical impedance spectroscopy. Int. J. Hydrog. Energy 2011, 36, 9815–9830.

53. Devrim, Y.; Albostan, A.; Devrim, H. Experimental investigation of CO tolerance in high temperature PEM fuel cells. Int. J. Hydrog. Energy 2018, 43, 18672–18681.

54. Oh, K.; Ju, H. Temperature dependence of CO poisoning in high-temperature proton exchange membrane fuel cells with phosphoric acid-doped polybenzimidazole membranes. Int. J. Hydrog. Energy 2015, 40, 7743–7753.

55. Jo, A.; Oh, K.; Lee, J.; Han, D.; Kim, D.; Kim, J.; Kim, B.; Kim, J.; Park, D.; Kim, M.; et al. Modeling and analysis of a 5 kWe HT-PEMFC system for residential heat and power generation. Int. J. Hydrog. Energy 2017, 42, 1698–1714.

56. Larminie, J.; Dicks, A.; McDonald, M.S. Fuel Cell Systems Explained; J. Wiley: Chichester, UK, 2003; Volume 2.

57. Authayanun, S.; Hacker, V. Energy and exergy analyses of a stand-alone HT-PEMFC based trigeneration system for residential applications. Energy Convers. Manag. 2018, 160, 230–242.

58. Tsatsaronis, G. Definitions and nomenclature in exergy analysis and exergoeconomics. Energy 2007, 32, 249–253.

59. Boyano, A.; Morosuk, T.; Blanco-Marigorta, A.M.; Tsatsaronis, G. Conventional and advanced exergoenvironmental analysis of a steam methane reforming reactor for hydrogen production. J. Clean. Prod. 2012, 20, 152–160.

60. Mert, S.O.; Ozcelik, Z.; Dincer, I. Comparative assessment and optimization of fuel cells. Int. J. Hydrog. Energy 2015, 40, 7835–7845.

61. Obara, S.; Tanno, I. Exergy analysis of a regional-distributed PEM fuel cell system. Int. J. Hydrog. Energy 2008, 33, 2300–2310.

62. BP Statistical Review of World Energy Statistical Review of World. Available online: https://www.bp.com/content/dam/bp/business-sites/en/global/corporate/pdfs/energy-economics/statistical-review/bp-stats-review-2019-natural-gas.pdf (accessed on 30 December 2019).

63. Methanex Monthly Average Regional Posted Contract Price History. Available online: https://www.methanex.com (accessed on 30 December 2019).